Beyond 20 Hz: Deriving the necessity of increased posting rates of unfocused SAR from first principles

Frithjof Ehlers*, Marcel Kleinherenbrink, Cornelis Slobbe, Martin Verlaan

* f.ehlers@tudelft.nl

CITG, TU Delft

Physical and Space Geodesy

TU Delft

Earlier studies

Dinardo Salvatore, Lucas Bruno, Benveniste Jerome. "Coastal and Inland Water SAR Altimetry at 80 Hz", OSTST 2015

Egido, Alejandro, Salvatore Dinardo, and Christopher Ray. "The Case for Increasing the Posting Rate in Delay/Doppler Altimeters." Advances in Space Research 68, no. 2 (July 2021): 930–36. https://doi.org/10.1016/j.asr.2020.03.014.

Buchhaupt, Christopher. "Model Improvement for SAR Altimetry." Technische Universität Darmstadt, 2019. http://oatd.org/oatd/record?record=oai%5C%3Atuprints.ulb.tu-darmstadt.de%5C%3A9015.

Rieu, P., T. Moreau, E. Cadier, M. Raynal, S. Clerc, C. Donlon, F. Borde, F. Boy, and C. Maraldi. "Exploiting the Sentinel-3 Tandem Phase Dataset and Azimuth Oversampling to Better Characterize the Sensitivity of SAR Altimeter Sea Surface Height to Long Ocean Waves." Advances in Space Research 67, no. 1 (January 2021): 253–65. https://doi.org/10.1016/j.asr.2020.09.037.

Precision improvement of 25% of geophysical estimates over ocean with 80 Hz sampling (and averaging to 20 Hz), altered SSH spectra and allowing to see finer scales over inland water targets.

Earlier studies

Dinardo Salvatore, Lucas Bruno, Benveniste Jerome. "Coastal and Inland Water SAR Altimetry at 80 Hz", OSTST 2015

Egido, Alejandro, Salvatore Dinardo, and Christopher Ray. "The Case for Increasing the Posting Rate in Delay/Doppler Altimeters." Advances in Space Research 68, no. 2 (July 2021): 930–36. https://doi.org/10.1016/j.asr.2020.03.014.

Buchhaupt, Christopher. "Model Improvement for SAR Altimetry." Technische Universität Darmstadt, 2019. http://oatd.org/oatd/record?record=oai%5C%3Atuprints.ulb.tu-darmstadt.de%5C%3A9015.

Rieu, P., T. Moreau, E. Cadier, M. Raynal, S. Clerc, C. Donlon, F. Borde, F. Boy, and C. Maraldi. "Exploiting the Sentinel-3 Tandem Phase Dataset and Azimuth Oversampling to Better Characterize the Sensitivity of SAR Altimeter Sea Surface Height to Long Ocean Waves." Advances in Space Research 67, no. 1 (January 2021): 253–65. https://doi.org/10.1016/j.asr.2020.09.037.

Precision improvement of 18-25% of geophysical estimates over ocean at 40 and 80 Hz posting rate (and averaging to 20 Hz).
Explanation: Waveform power speckle decorrelates faster (150 m) in along-track direction than predicted from 300 m resolution.

Earlier studies

Dinardo Salvatore, Lucas Bruno, Benveniste Jerome. "Coastal and Inland Water SAR Altimetry at 80 Hz", OSTST 2015

Egido, Alejandro, Salvatore Dinardo, and Christopher Ray. "The Case for Increasing the Posting Rate in Delay/Doppler Altimeters." Advances in Space Research 68, no. 2 (July 2021): 930–36. https://doi.org/10.1016/j.asr.2020.03.014.

Buchhaupt, Christopher. "Model Improvement for SAR Altimetry." Technische Universität Darmstadt, 2019. http://oatd.org/oatd/record?record=oai%5C%3Atuprints.ulb.tu-darmstadt.de%5C%3A9015.

Rieu, P., T. Moreau, E. Cadier, M. Raynal, S. Clerc, C. Donlon, F. Borde, F. Boy, and C. Maraldi. "Exploiting the Sentinel-3 Tandem Phase Dataset and Azimuth Oversampling to Better Characterize the Sensitivity of SAR Altimeter Sea Surface Height to Long Ocean Waves." Advances in Space Research 67, no. 1 (January 2021): 253–65. https://doi.org/10.1016/j.asr.2020.09.037.

Slight precision improvement of SSH over ocean with 40 Hz sampling.
Explanation: Due to power detection, the point target response (PTR) contains twice the bandwidth, hence oversampling is needed.

Earlier studies

Dinardo Salvatore, Lucas Bruno, Benveniste Jerome. “Coastal and Inland Water SAR Altimetry at 80 Hz”, OSTST 2015

Egido, Alejandro, Salvatore Dinardo, and Christopher Ray. “The Case for Increasing the Posting Rate in Delay/Doppler Altimeters.” Advances in Space Research 68, no. 2 (July 2021): 930–36. https://doi.org/10.1016/j.asr.2020.03.014.

Buchhaupt, Christopher. “Model Improvement for SAR Altimetry.” Technische Universität Darmstadt, 2019. http://oatd.org/oatd/record?record=oai%5C%3Atuprints.ulb.tu-darmstadt.de%5C%3A9015.

Rieu, P., T. Moreau, E. Cadier, M. Raynal, S. Clerc, C. Donlon, F. Borde, F. Boy, and C. Maraldi. “Exploiting the Sentinel-3 Tandem Phase Dataset and Azimuth Oversampling to Better Characterize the Sensitivity of SAR Altimeter Sea Surface Height to Long Ocean Waves.” Advances in Space Research 67, no. 1 (January 2021): 253–65. https://doi.org/10.1016/j.asr.2020.09.037.

There are high frequencies in the SSH signal related to swell, which can only be detected with 80 (or at least 40) Hz sampling rate, but are otherwise aliased with the 20 Hz product.

Questions for this talk

Can we calculate the optimal posting rate for UF-SAR?

1. Can we calculate the speckle autocorrelation of the waveform power?
2. What are expected improvements of e.g. SSH estimates (precision / sampling)?

Multilooked point target response

The PTR of the UF-SAR power from a single Doppler beam index l in range gate k is approximated by (Ray et al., 2015):

$$h^2(k,l) \approx C\mathrm{sinc}^2\left[\frac{x}{L_x} - l\right]\mathrm{sinc}^2\left[k - k_l\right],$$

In the focused radargram the point target appears tilted with increasing looking angle of the Doppler beam:

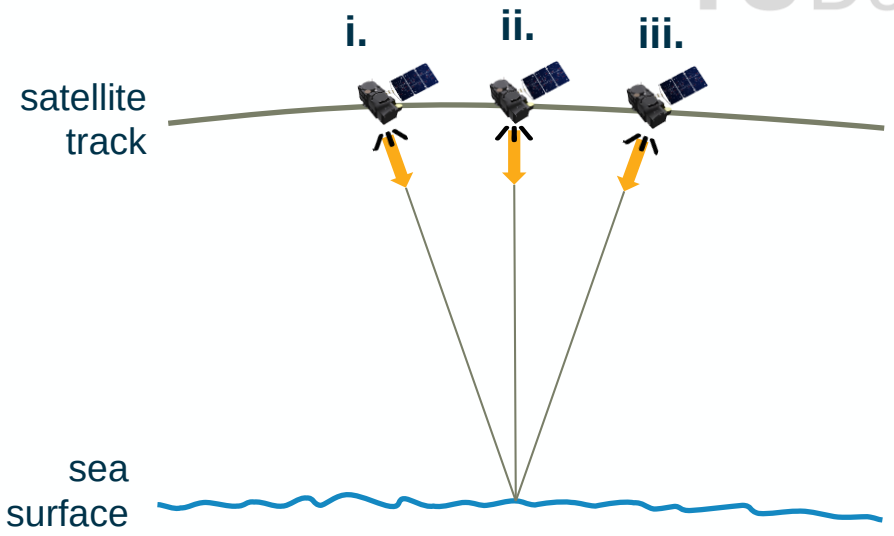

Multilooked point target response

The PTR of the UF-SAR power from a single Doppler beam index l in range gate k is approximated by (Ray et al., 2015):

$$h^2(k,l) \approx C\mathrm{sinc}^2\left[\frac{x}{L_x} - l\right]\mathrm{sinc}^2\left[k - k_l\right],$$

In the focused radargram the point target appears tilted with increasing looking angle of the Doppler beam:

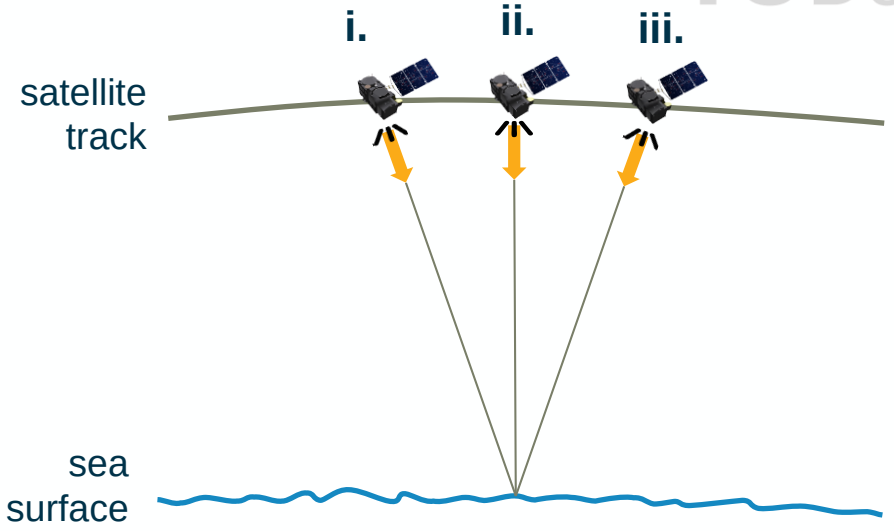

i. point target as seen by *forward looking* Doppler beam

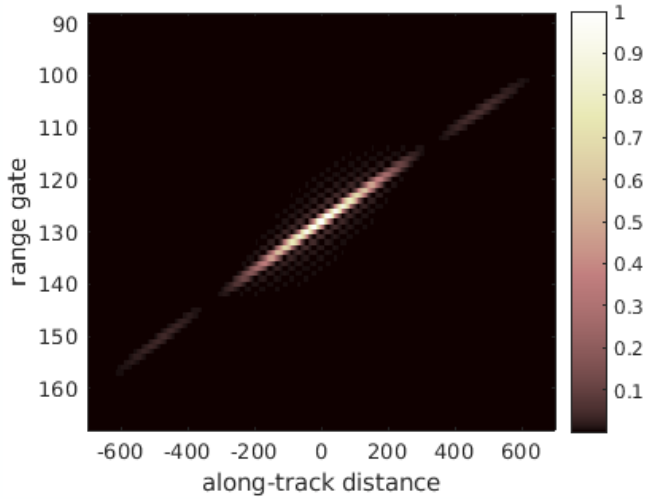

ii. point target as seen by *nadir looking* Doppler beam

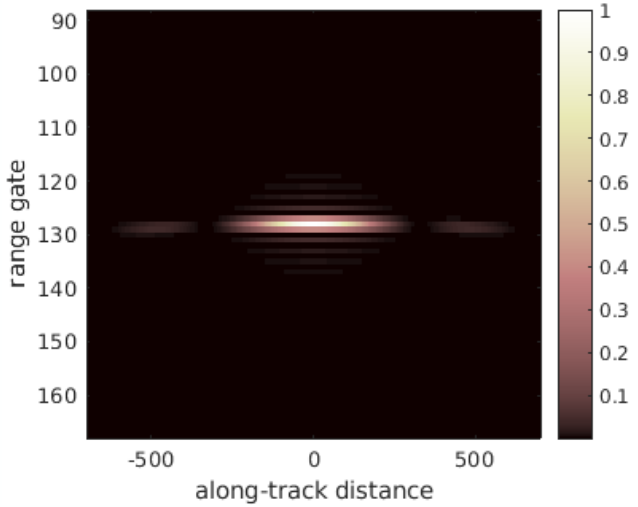

iii. point target as seen by *backward looking* Doppler beam

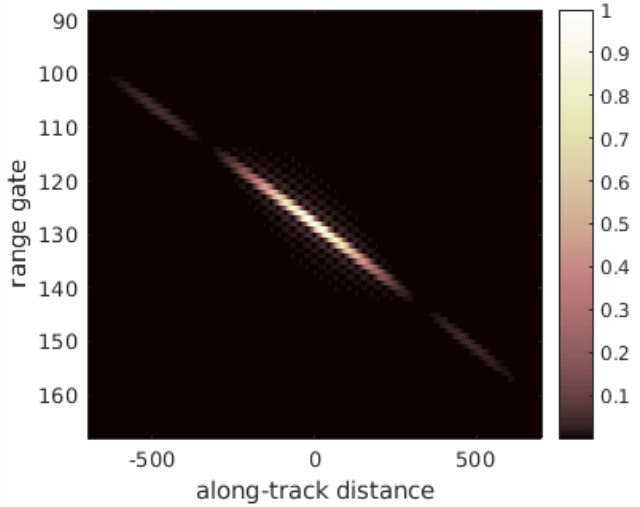

Multilooked point target response

The PTR of the UF-SAR power from a single Doppler beam index l in range gate k is approximated by (Ray et al., 2015):

$$h^2(k,l) \approx C\mathrm{sinc}^2\left[\frac{x}{L_x} - l\right]\mathrm{sinc}^2\left[k - k_l\right],$$

After multilooking (adding up all Doppler beams) we end up with a characteristic bow-tie pattern:

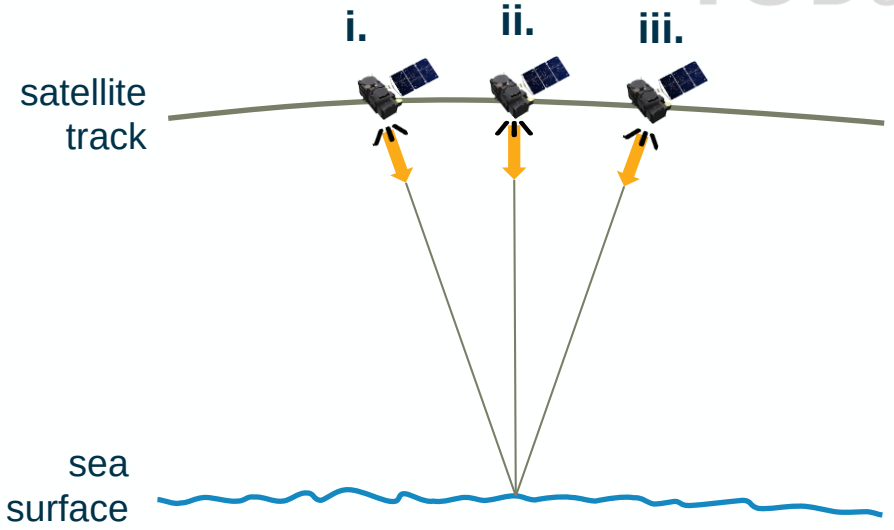

point target as seen in the *multilooked* radargram

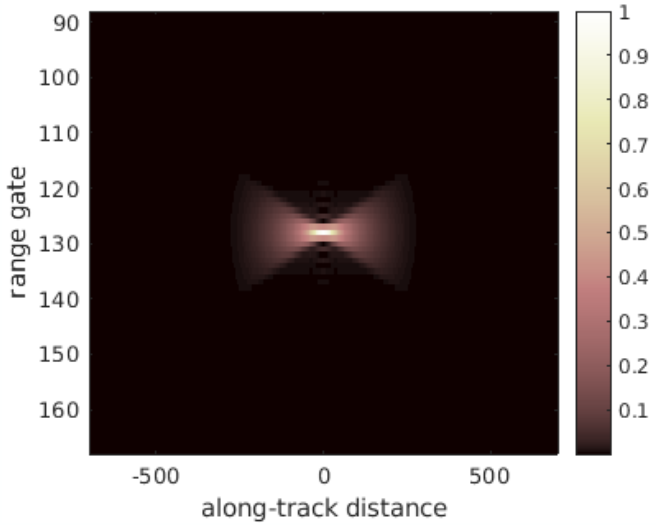

Multilooked point target response

The PTR of the UF-SAR power from a single Doppler beam index l in range gate k is approximated by (Ray et al., 2015):

$$h^2(k,l) \approx C\mathrm{sinc}^2\left[\frac{x}{L_x} - l\right]\mathrm{sinc}^2\left[k - k_l\right],$$

After multilooking (adding up all Doppler beams) we end up with a characteristic bow-tie pattern:

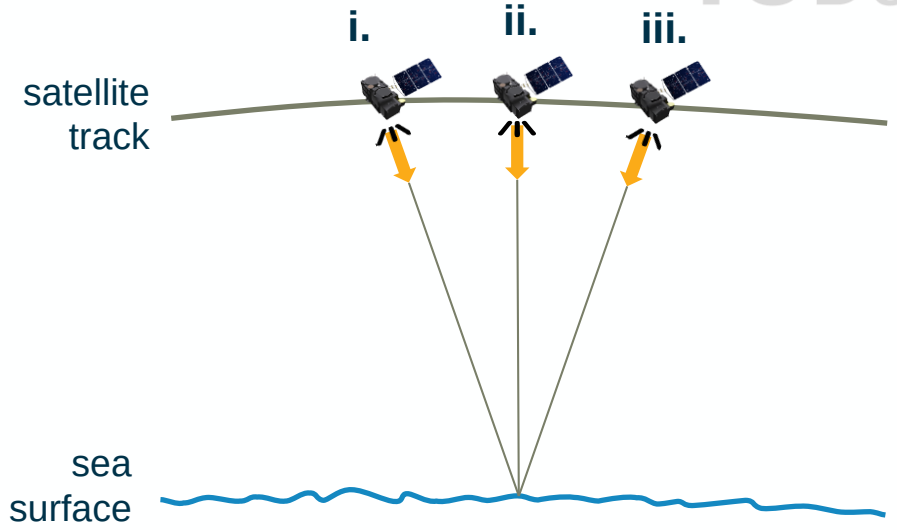

point target as seen in the *multilooked* radargram

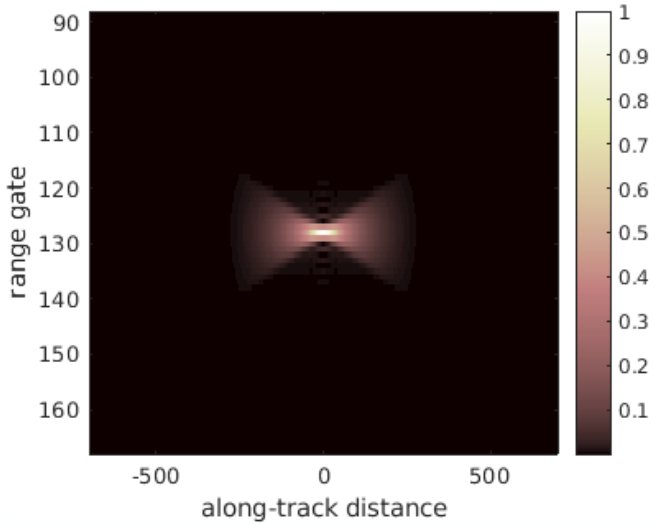

$$h_{\mathrm{m}}^2(r,x) \approx C\mathrm{sinc}^2\left[\frac{x}{L_x}\right]\sum_{t_b} G_x^2(Vt_b)\,\mathrm{sinc}^2\left[\frac{2B}{c}(r - r_b)\right]$$

with

$$r_b = \frac{xV}{H}t_b + \frac{x^2}{2H} + \frac{y^2}{2H} - z - \frac{xf_cV}{Hs}$$

Speckle noise autocorrelation function ~ PTR

Over ocean, the speckle noise autocorrelation function of the waveform power is dominated by / provided by the PTR as shown here below:

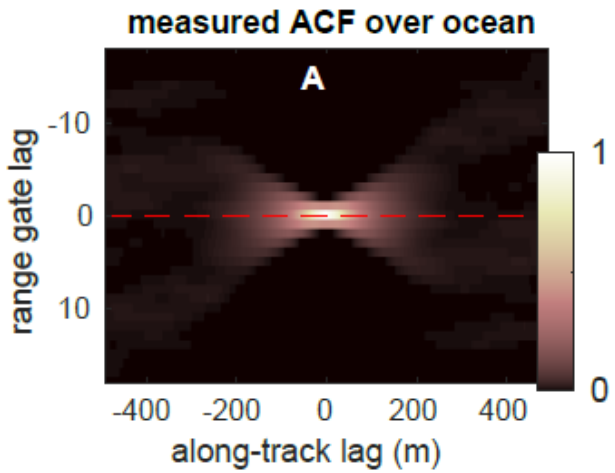

Speckle noise autocorrelation function ~ PTR

Over ocean, the speckle noise autocorrelation function of the waveform power is dominated by / provided by the PTR as shown here below:

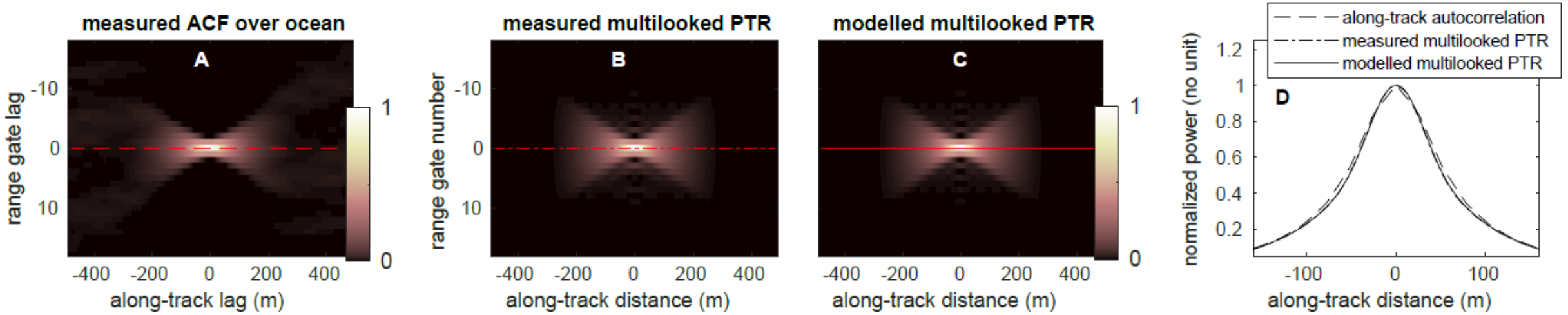

Multilooked point target response

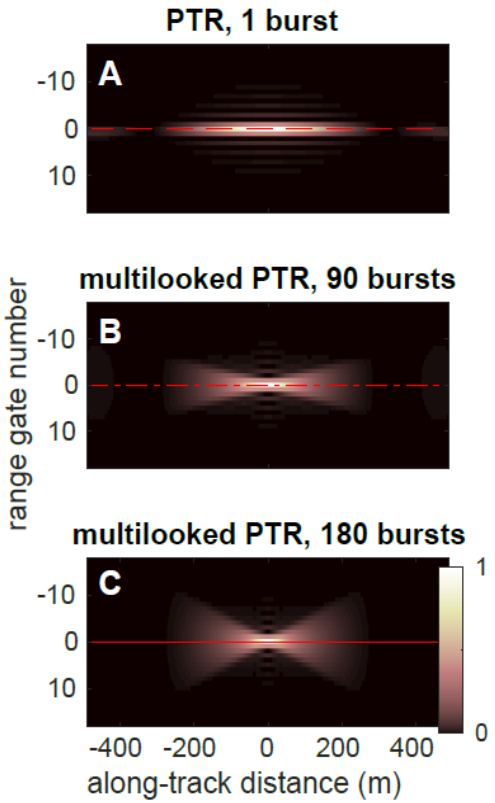

A-C: The summing of multiple Doppler beams spreads the power over multiple range bins.

Multilooked point target response

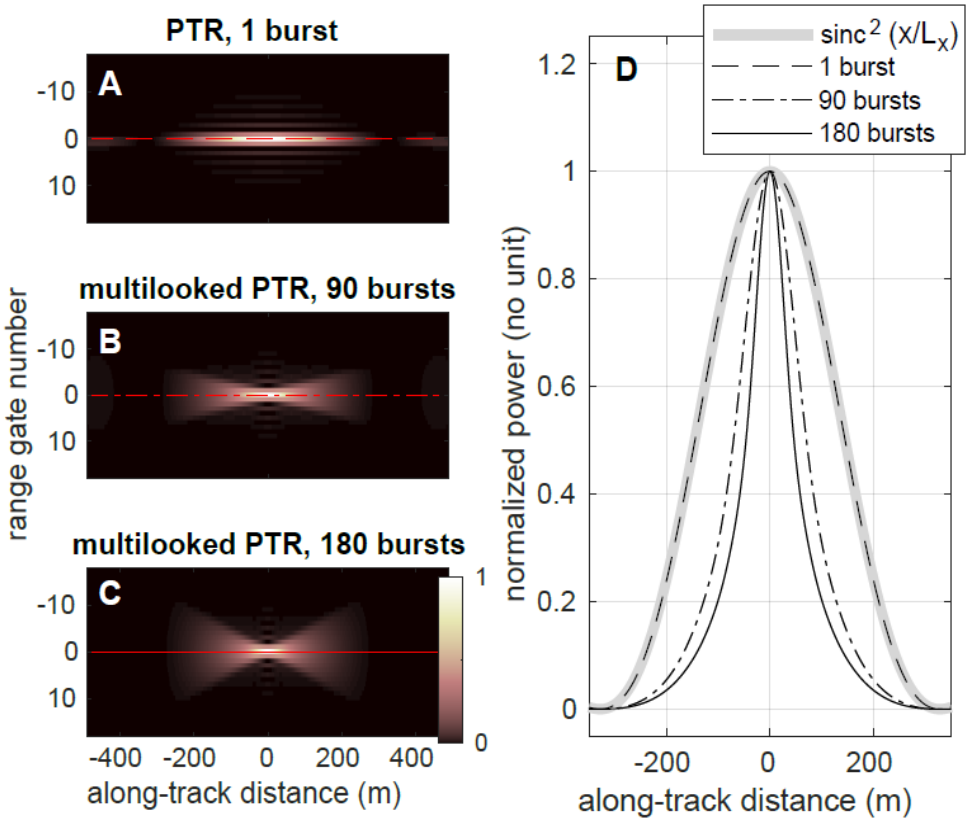

A-C: The summing of multiple Doppler beams spreads the power over multiple range bins.

D: Hence, the PTR appears narrower than the sinc^2 function when looking only in the along-track direction (power along the red lines from panels A-C plotted in D).

Multilooked point target response

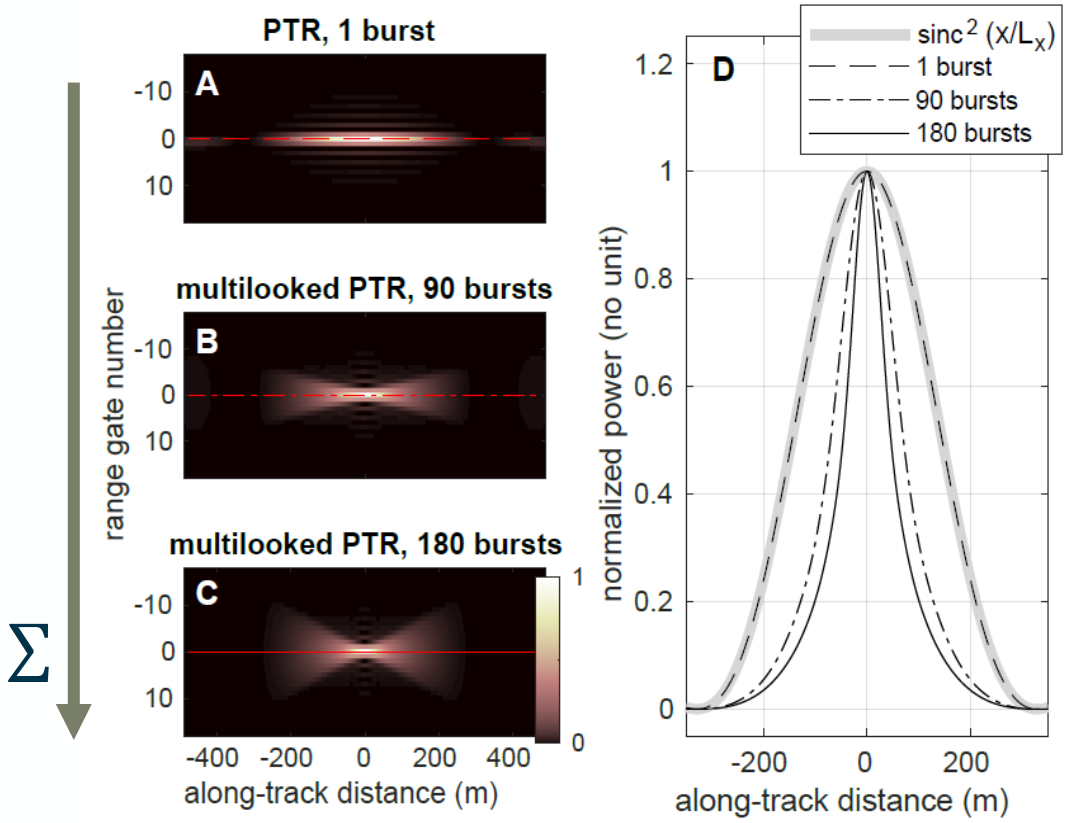

For A, B and C:

$$\sum_r p_r = \mathrm{C}\ \mathrm{sinc}^2\left(\frac{x}{L_x}\right)$$

A-C: The summing of multiple Doppler beams spreads the power over multiple range bins.

D: Hence, the PTR appears narrower than the sinc^2 function when looking only in the along-track direction (power along the red lines from panels A-C plotted in D).

However, once we sum the patterns in panels A-C over the range, we retrieve the well-known sinc^2 term again.

Noise autocorrelation functions of waveform power and SSH

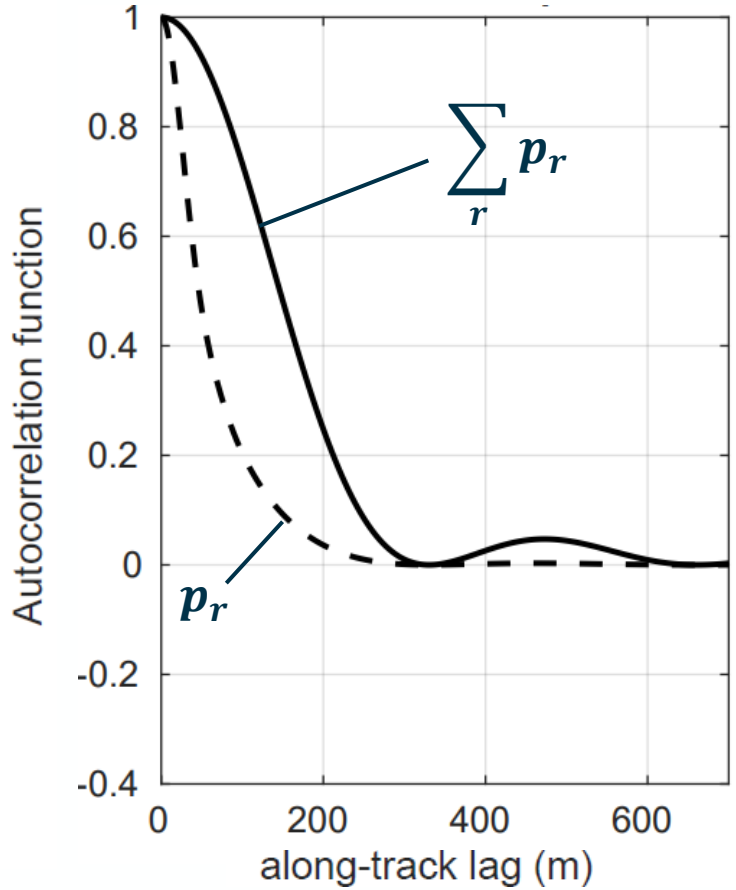

Noise autocorrelation functions of waveform power and SSH

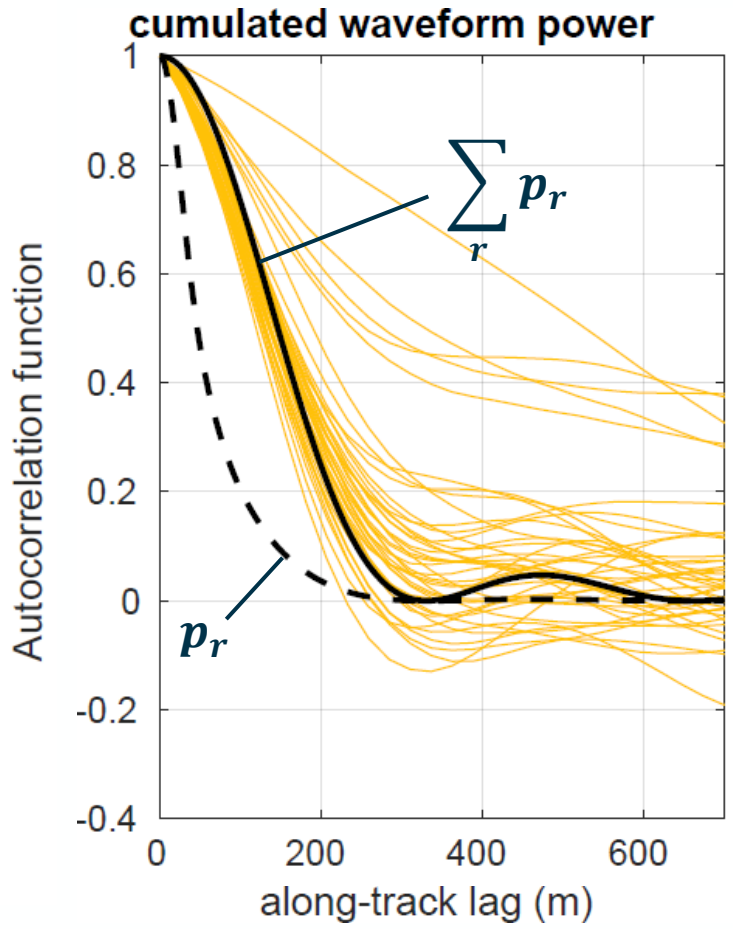

Noise autocorrelation functions of waveform power and SSH

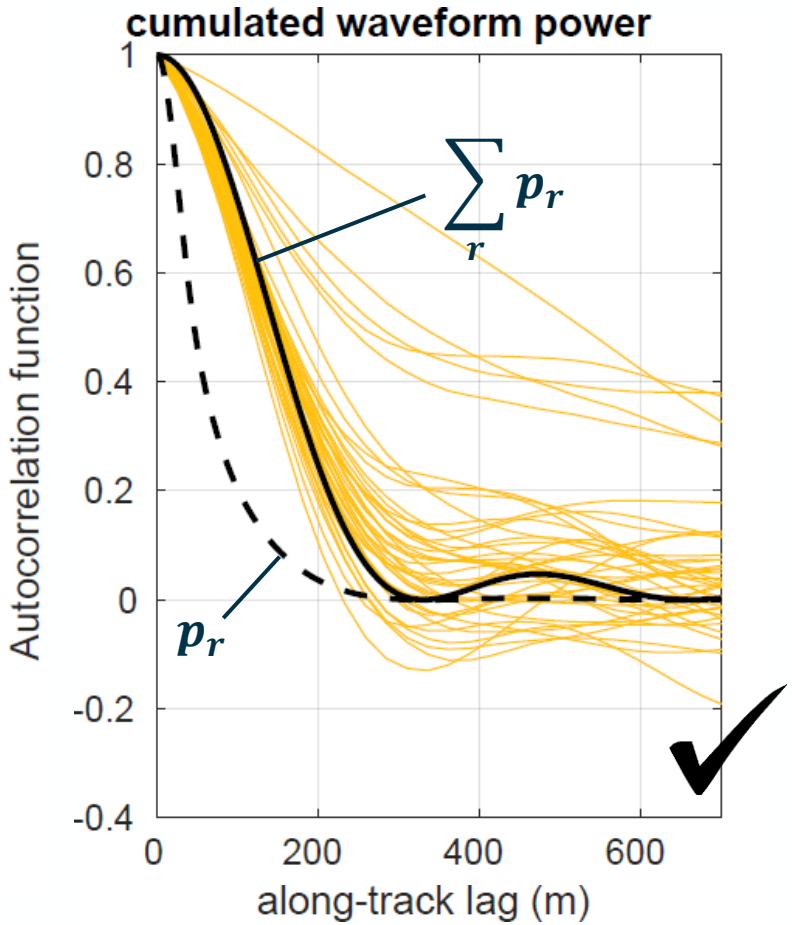

Noise autocorrelation functions of waveform power and SSH

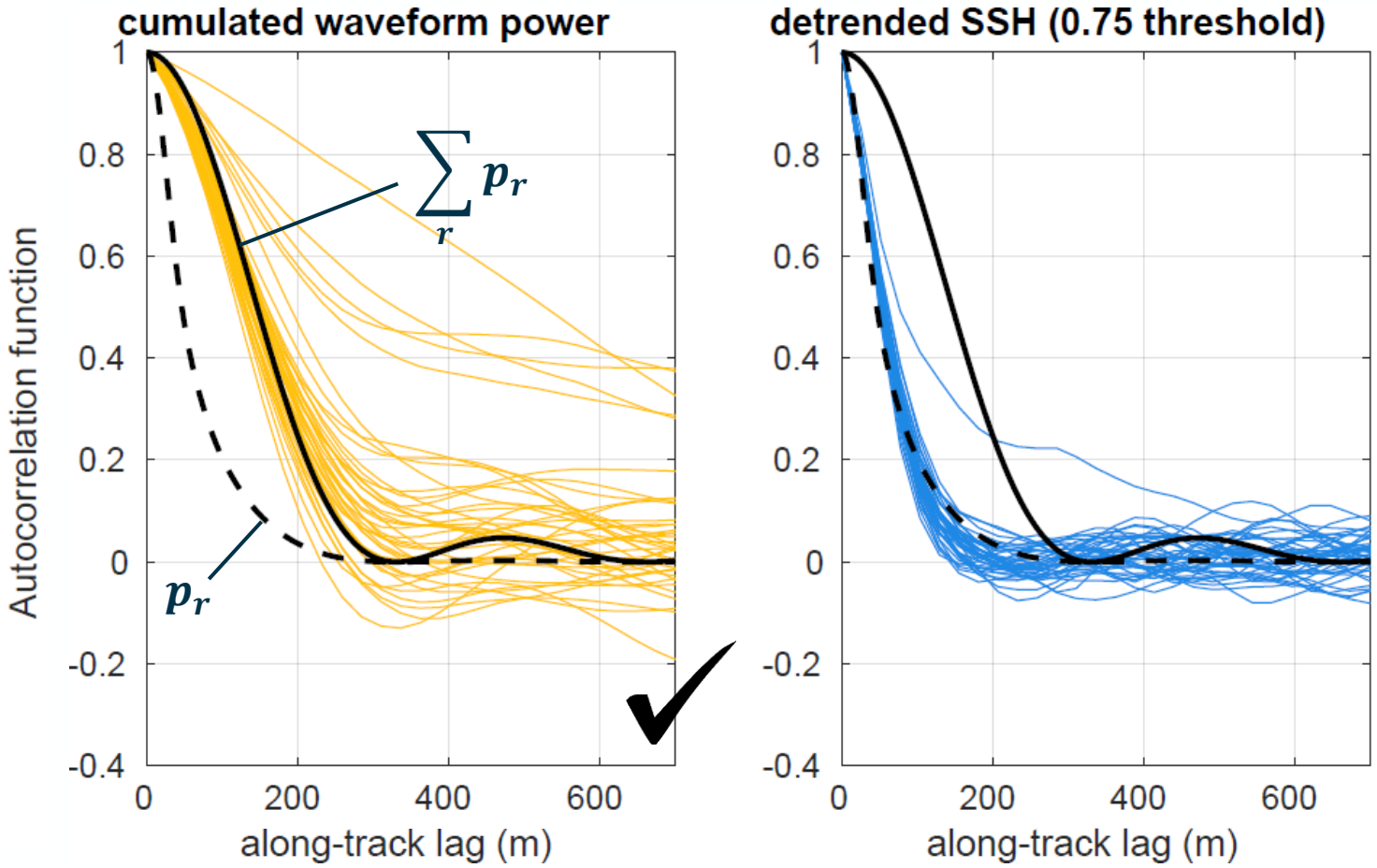

Noise autocorrelation functions of waveform power and SSH

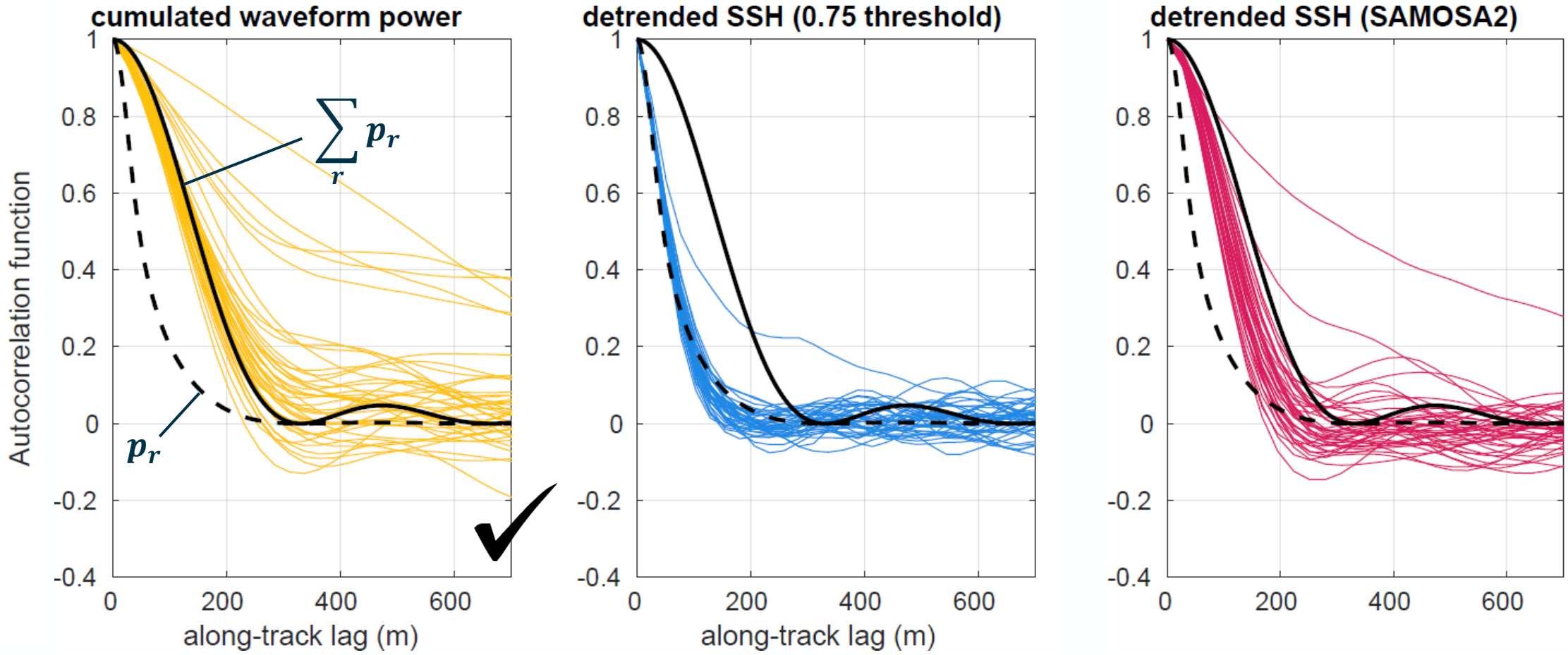

Noise autocorrelation functions of waveform power and SSH

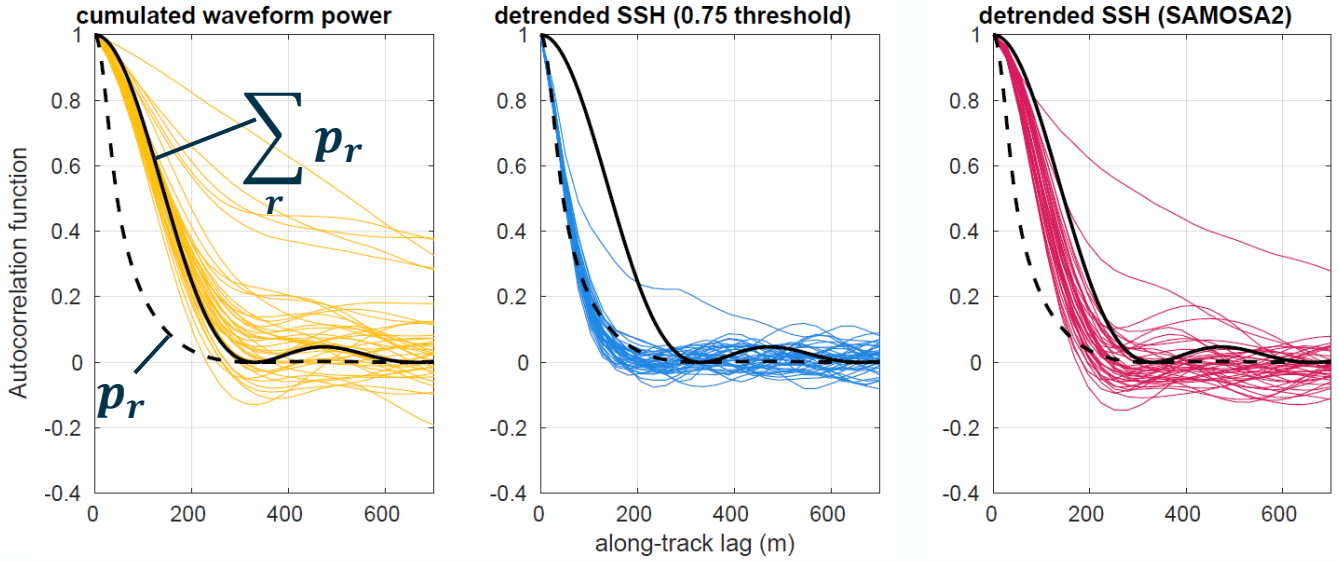

i) The SSH noise correlation length and therefore the required posting rate of UF-SAR is retracker dependent!

Noise autocorrelation functions of waveform power and SSH

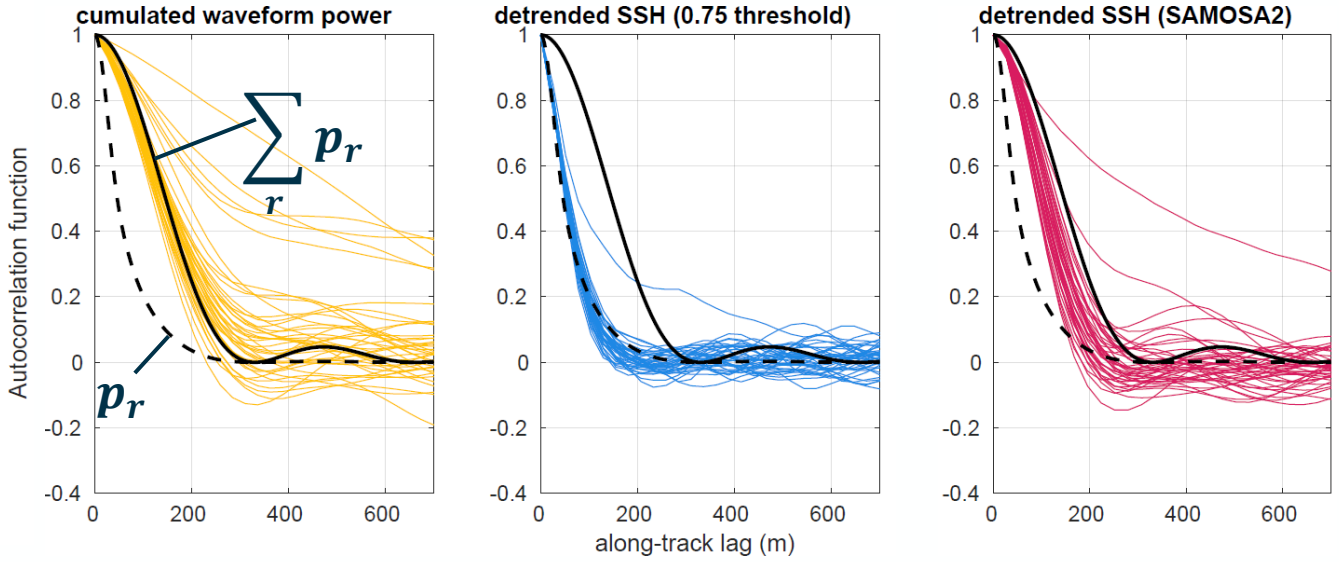

i) The SSH noise correlation length and therefore the required posting rate of UF-SAR is retracker dependent!

ii) The threshold retracker considers power values from at most 3 range gates, hence its range estimates decorrelate similar to the power in a single range gate.

$ACF(SSH) \approx ACF(p_r)$

Noise autocorrelation functions of waveform power and SSH

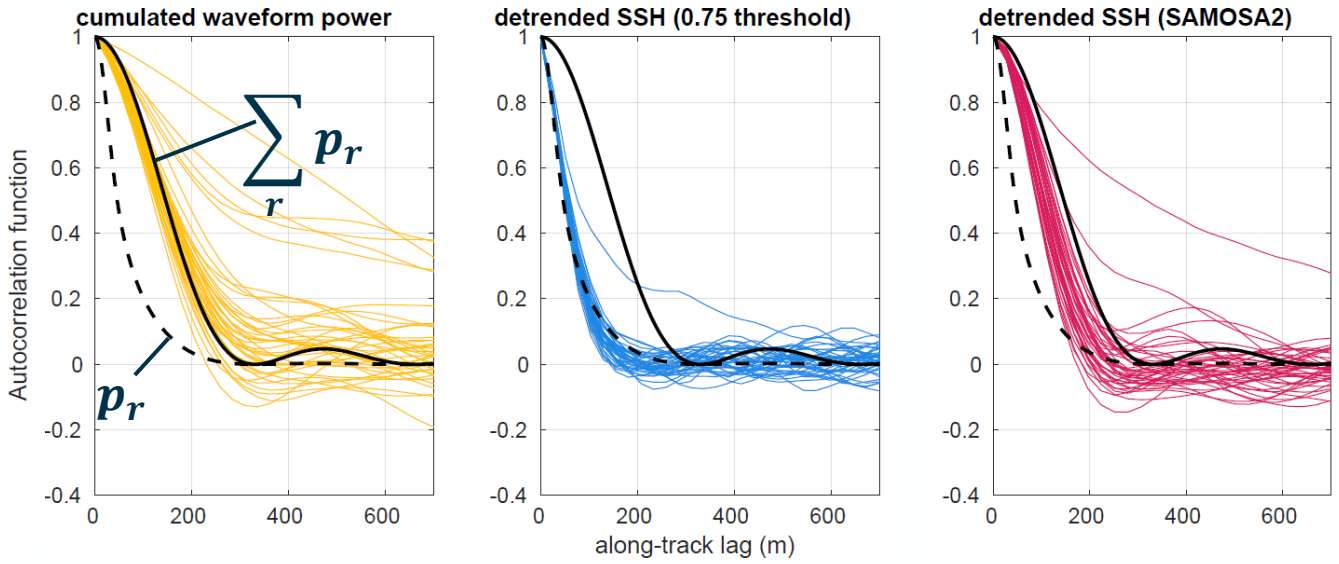

i) The SSH noise correlation length and therefore the required posting rate of UF-SAR is retracker dependent!

ii) The threshold retracker considers power values from at most 3 range gates, hence its range estimates decorrelate similar to the power in a single range gate.

$$ACF(SSH) \approx ACF(p_r)$$

iii) The noise of the SAMOSA2 retracker estimates can be written as a weighted sum over all power values (in a linearisation) and therefore decorrelates much slower than the signal in a single range gate p_r.

$$ACF(SSH) \approx ACF(\Sigma w_r p_r) \sim ACF(\Sigma p_r)$$

Where do the improvements come from then?

i) Precision:

In reality noise and signal cannot be well seperated:

Here we use synthetic gaussian noise at 80 Hz sampling with sinc^2 autocorrelation corresponding to a 20 Hz resolution.

Where do the improvements come from then?

i) Precision:

In reality noise and signal cannot be well seperated:

Here we use synthetic gaussian noise at 80 Hz sampling with sinc^2 autocorrelation corresponding to a 20 Hz resolution.

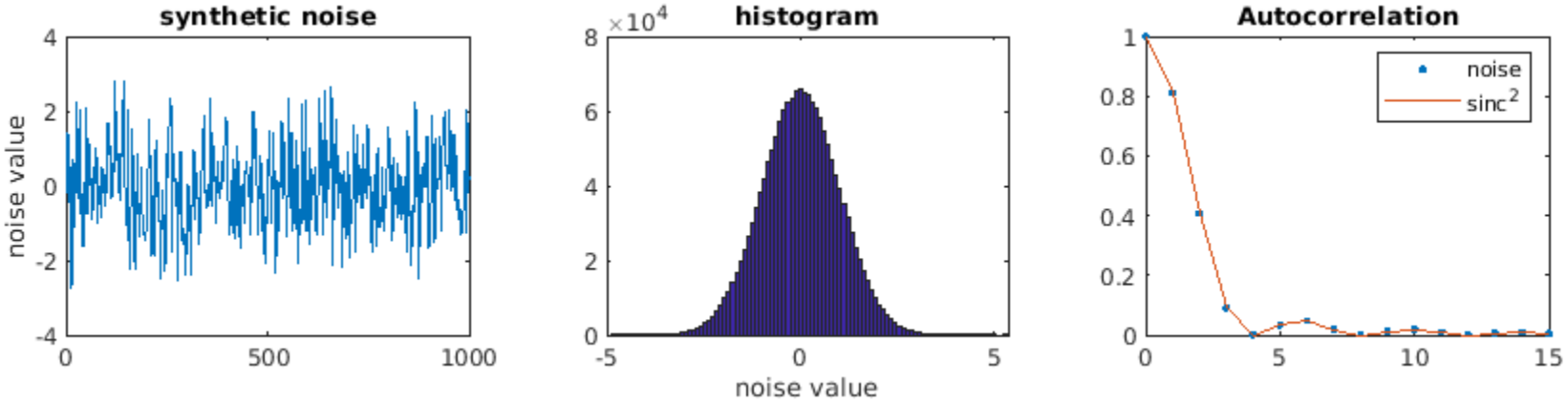

Where do the improvements come from then?

Precision:

In reality noise and signal cannot be well seperated:

Here we use synthetic gaussian noise at 80 Hz sampling with sinc^2 autocorrelation corresponding to a 20 Hz resolution.

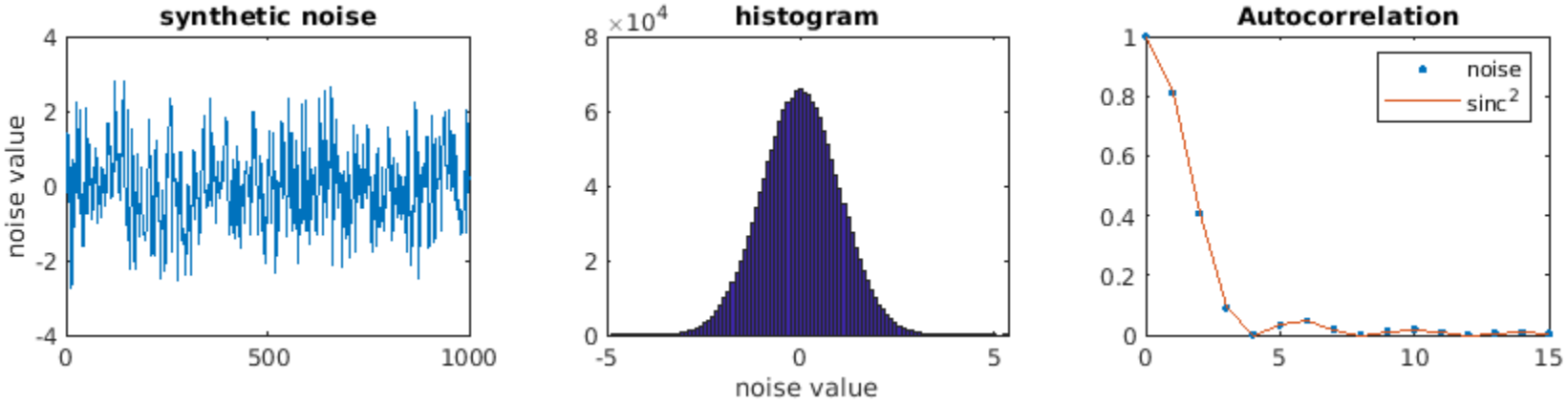

	subsampling to 20 Hz	averaging 80 Hz to 20 Hz
noise standard deviation	1	0.81
noise correlation between consecutive 20 Hz samples	0	0.195

Where do the improvements come from then?

Precision:

In reality noise and signal cannot be well seperated:

Here we use synthetic gaussian noise at 80 Hz sampling with $sinc^2$ autocorrelation corresponding to a 20 Hz resolution.

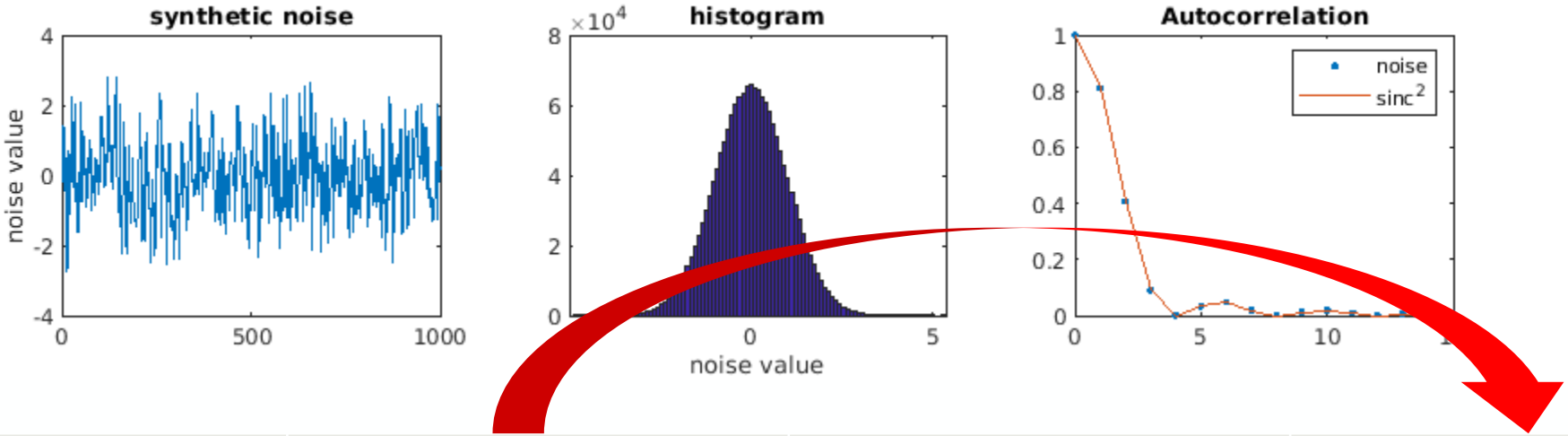

	subsampling to 20 Hz	averaging 80 Hz to 20 Hz	**"filtered" 20 Hz** (with appropriate averaging kernel)
noise standard deviation	1	0.81	**0.81**
noise correlation between consecutive 20 Hz samples	0	0.195	**0.195**

Where do the improvements come from then?

Precision:

In reality noise and signal cannot be well seperated:

Here we use synthetic gaussian noise at 80 Hz sampling with $sinc^2$ autocorrelation corresponding to a 20 Hz resolution.

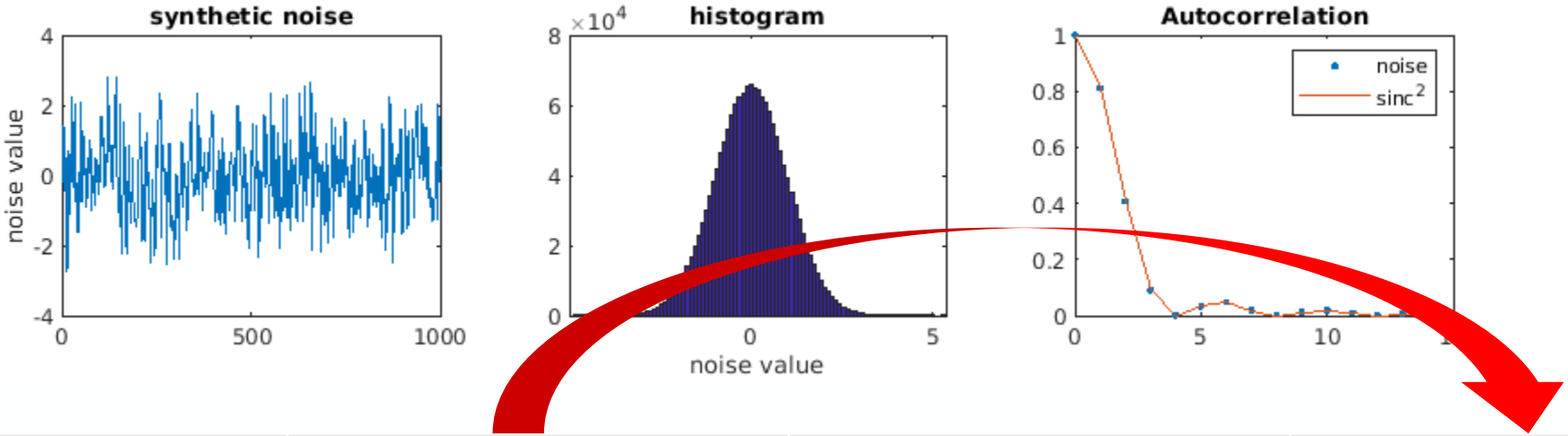

	subsampling to 20 Hz	averaging 80 Hz to 20 Hz	**"filtered" 20 Hz** (with appropriate averaging kernel)
noise standard deviation	1	0.81	**0.81**
noise correlation between consecutive 20 Hz samples	0	0.195	**0.195**

In this example, the precision improvement is a mere artifact of the increased point-to-point correlation!

Where do the improvements come from then?

Precision:

In a real data comparison of Sentinel-3 UF-SAR vs. FF-SAR we see the same tendency.

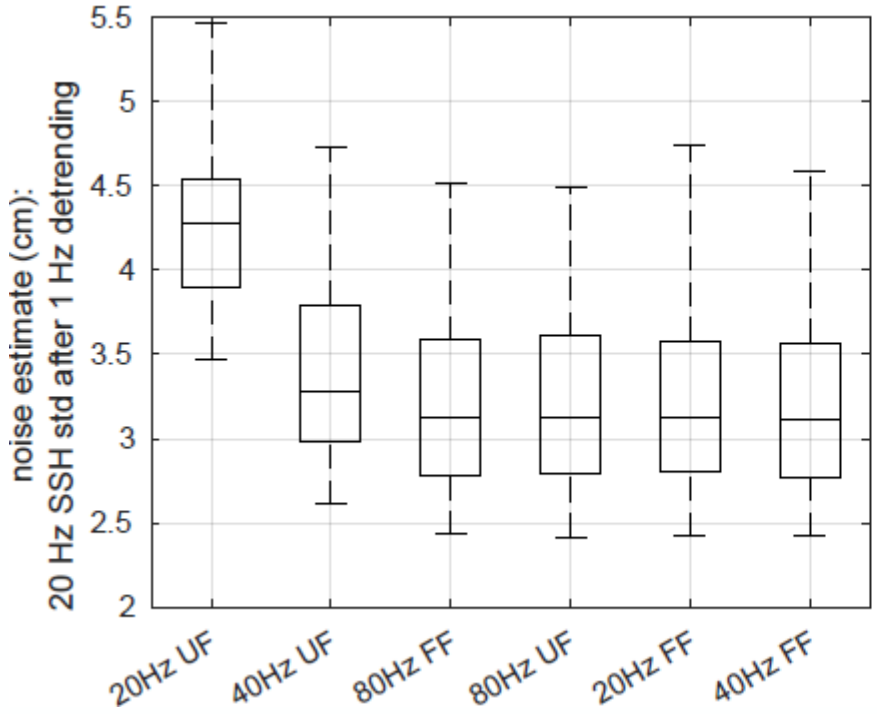

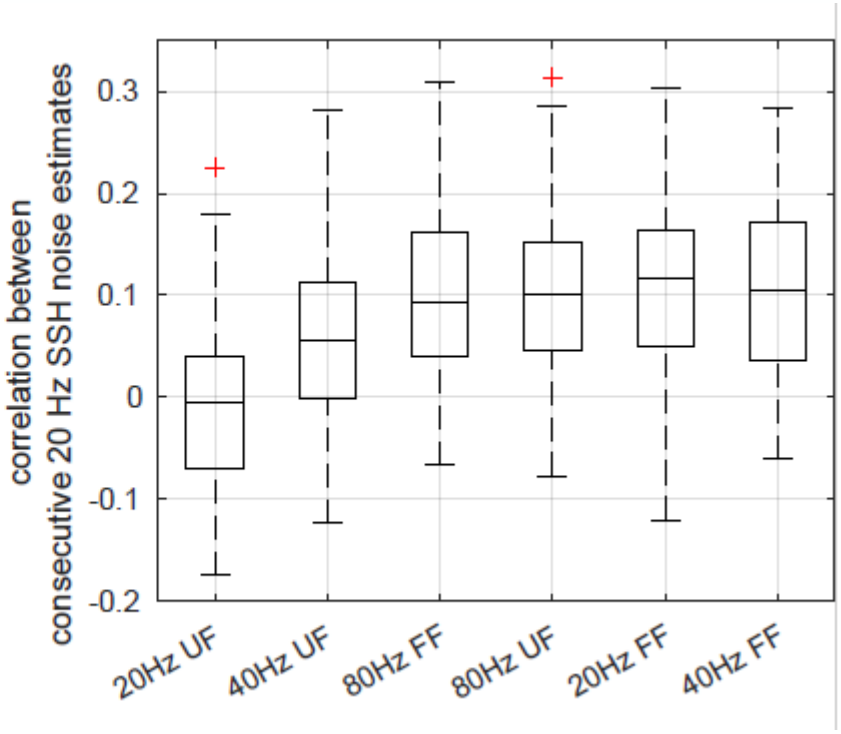

Where do the improvements come from then?

Precision:

In a real data comparison of Sentinel-3 UF-SAR vs. FF-SAR we see the same tendency.

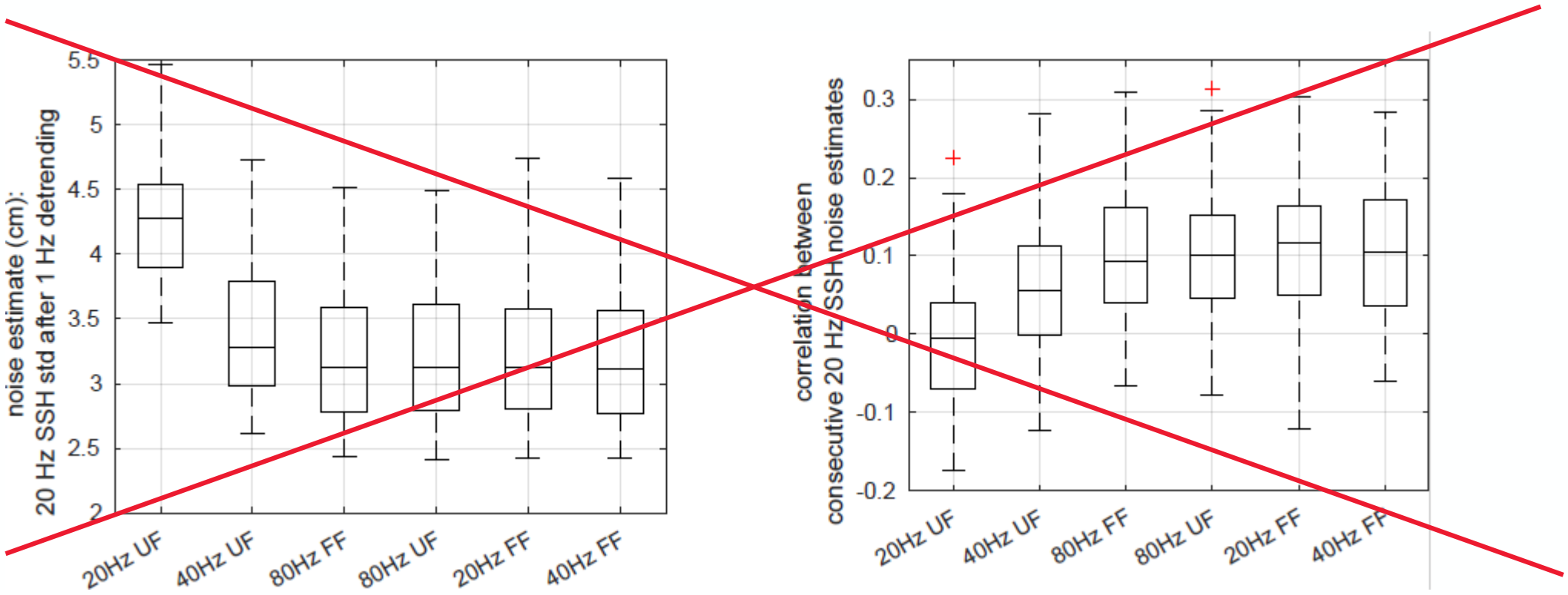

Estimates not comparable to UF-SAR 20 Hz unless "pre-whitened"
or post-processed otherwise!

Noise spectrum at differen posting rates

Forming the noise spectral densities yields white noise for 20 Hz and colored noise for 40 and 80 Hz, but the noise standard deviation is identical for all! These noise tails are in agreement with earlier studies.

Due to squaring (power detection) the highest frequency is 20 Hz, hence at least 40 Hz sampling is required in order not to alias power.

This is similar to the required zero-padding of the waveforms in range direction, see

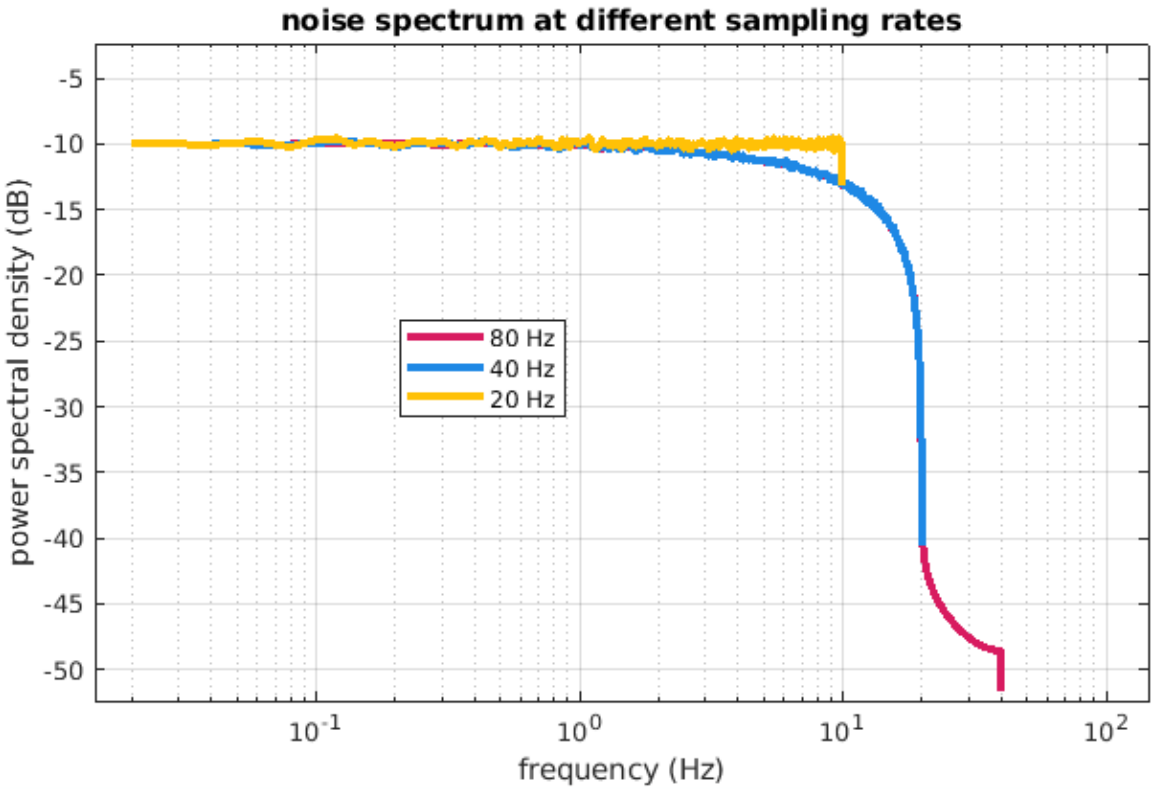

Smith, Walter H. F., and Remko Scharroo. "Waveform Aliasing in Satellite Radar Altimetry." IEEE Transactions on Geoscience and Remote Sensing 53, no. 4 (April 2015): 1671–82. https://doi.org/10.1109/TGRS.2014.2331193.

Take-home messages

- The radargram contains power peaks that are much narrower in along-track direction than 300 m (namely ~100m), hence oversampling for inland waters is suggested.

- The along-track noise autocorrelation over ocean is different for different variables and retrackers.
  - Higher sampling not necessarily reasonable.
  - The effective number of looks (ENL) along a single range gate is not necessarily representative for performance!

- The referenced studies did not report / quantify the correlation between consecutive 20 Hz samples. This may have led to overly optimistic performance estimates of 40 and 80 Hz products!

- At least 40 Hz posting rate is needed to compute unaliased spectra in case of a perfect sinc^2 decorrelation behaviour.

Backup slides

Posting rate estimates based on FWHM?

Considering the Full Width at Half Maximum (FWHM) of the $sinc^2$ against the actual decorrelation, we can make a rough estimate the required posting rates over ocean in dependence of the used number of Doppler beams.

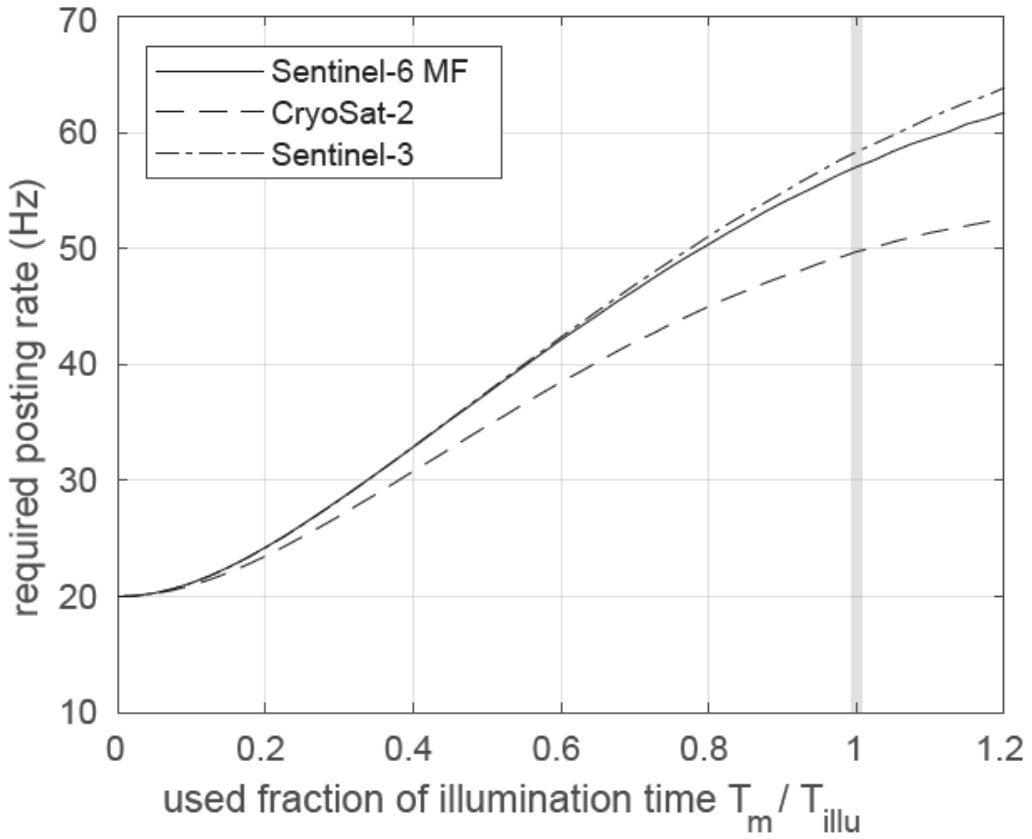

Posting rate estimates based on FWHM?

Considering the Full Width at Half Maximum (FWHM) of the $sinc^2$ against the actual decorrelation, we can make a rough estimate the required posting rates over ocean in dependence of the used number of Doppler beams.

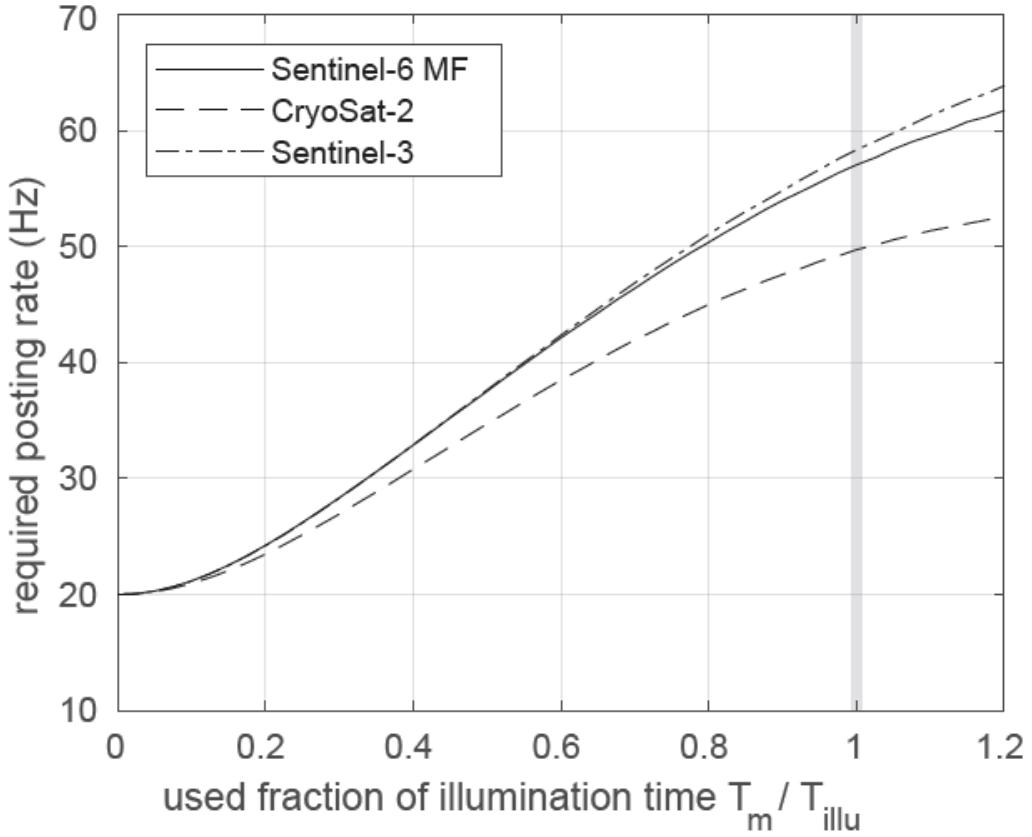

However, that is only true when looking from a single range bin and ignoring the 2D structure!
But what about estimates like SSH?

Noise autocorrelation functions of waveform power and SSH

Methodology

- Process UF-SAR waveforms with 240 Hz posting rate
- Retrack UF-SAR range on ~240 Hz with SAMOSA2 and threshold retracker (0.75)
- Detrend the uncorrected SSH = altitude - retracked range with 1 Hz moving median and remove outliers via MAD. The residual should be dominated by noise.
- Calculate noise ACFs

Waveforms

return signal over open ocean

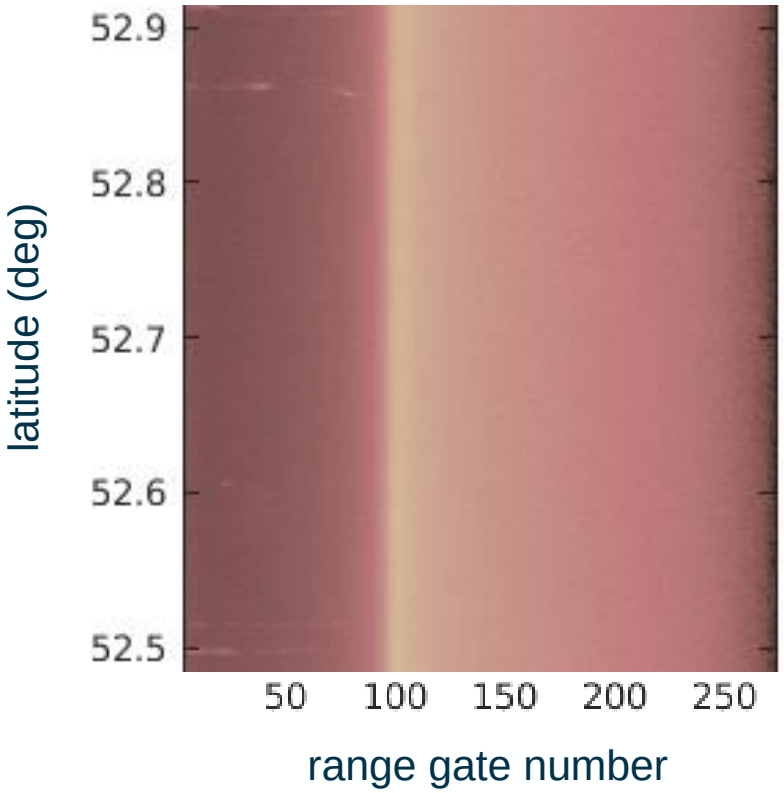

return signal over coastal zone

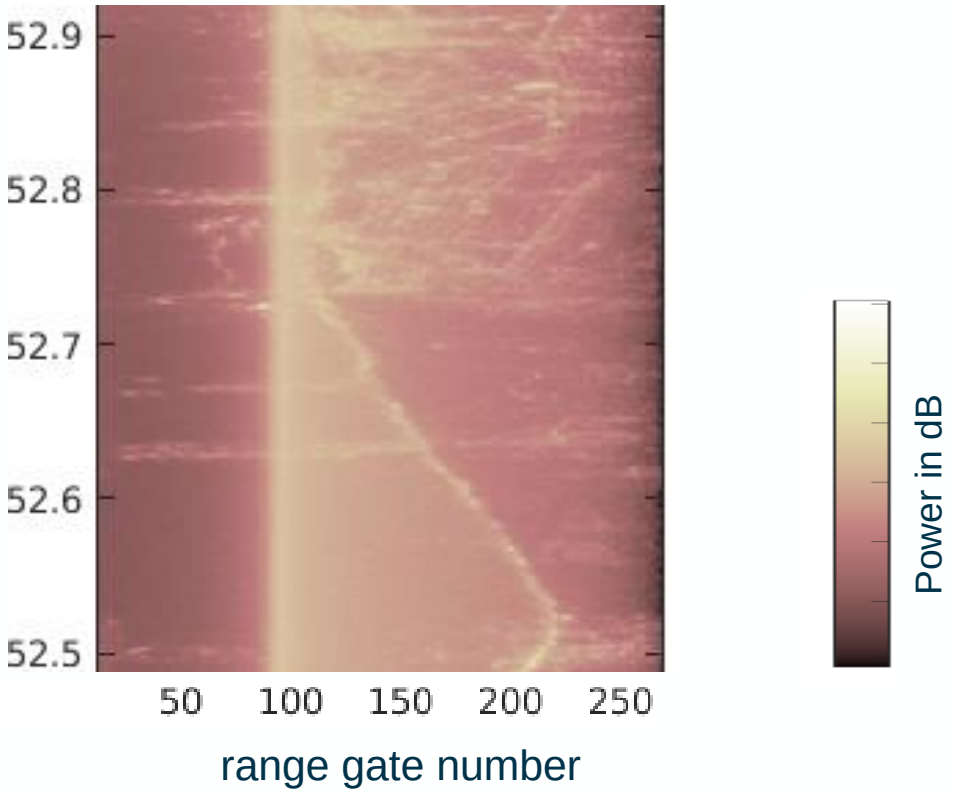

Closed-burst and open-burst operations

CryoSat-2
Sentinel-3

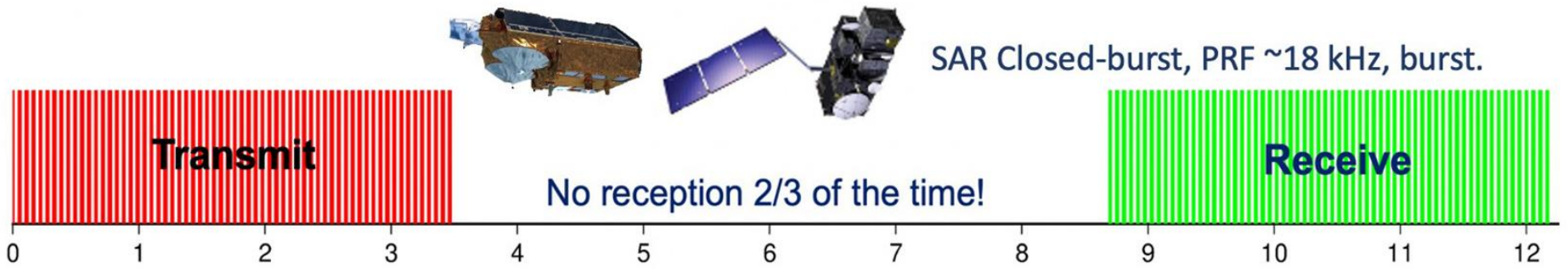

Sentinel-6 MF

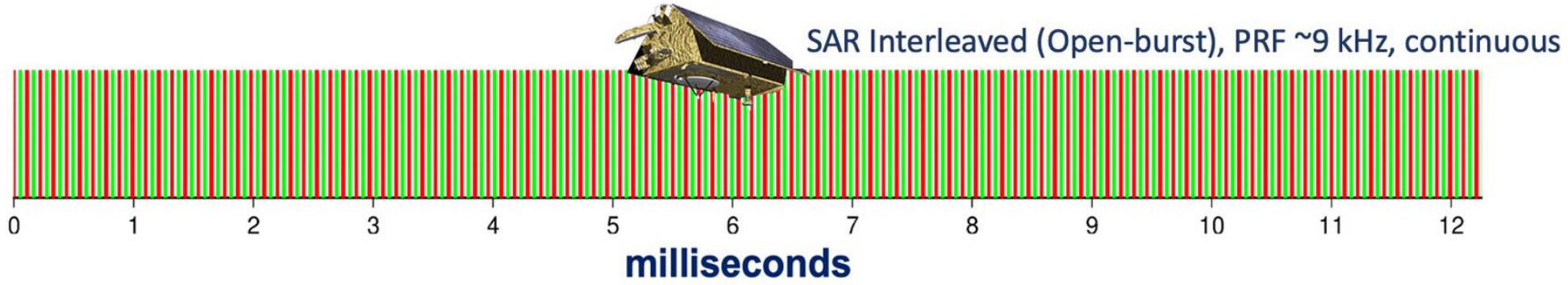

Donlon et al. (2021), doi.org/10.1016/j.rse.2021.112395

Synthetic aperture and along-track resolution

Here, a toy model of how measurement gaps cause frequency duplicates (grating lobes)

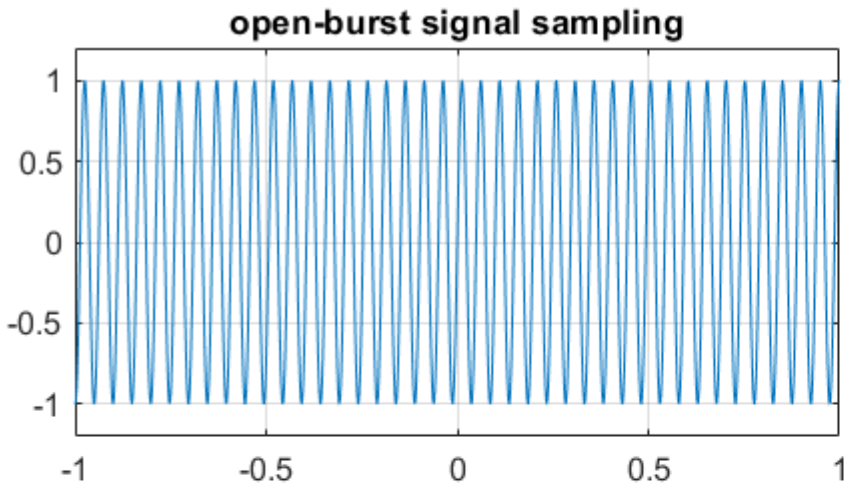

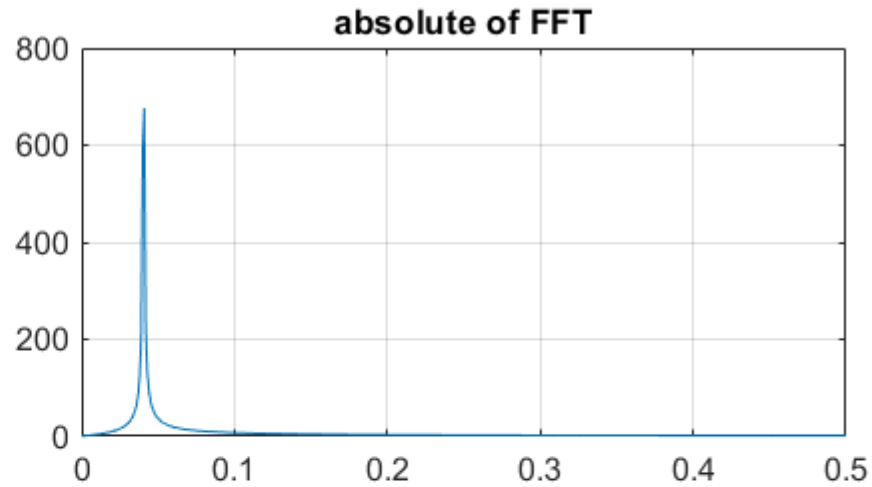

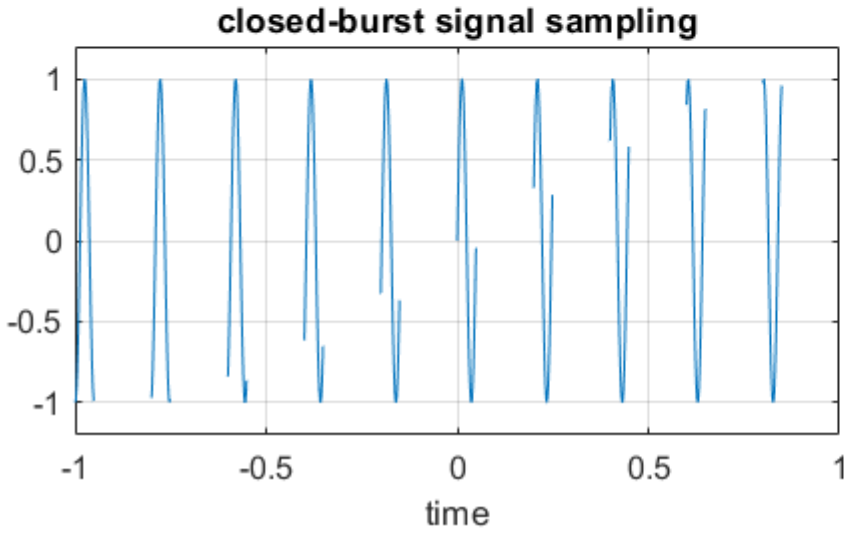

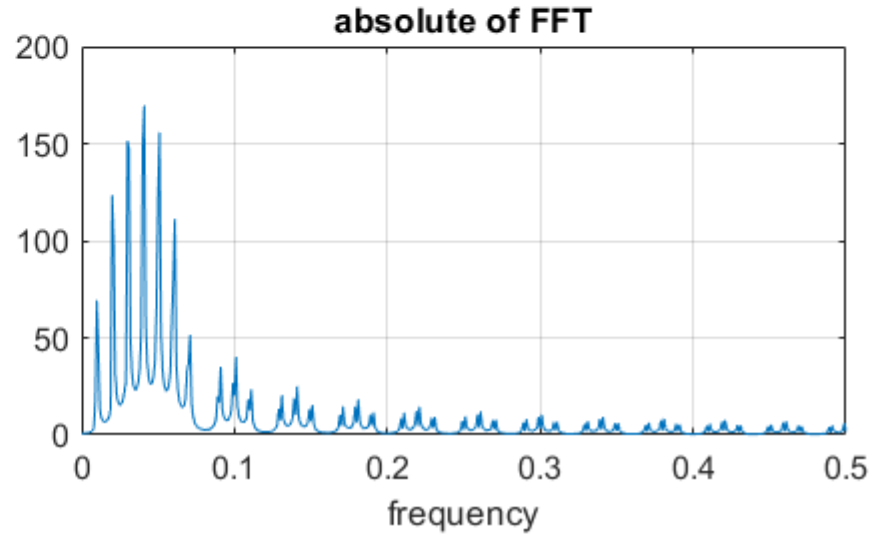

$$h^2_{\mathrm{FF}}(r,x) = h^2_{\mathrm{FF}}(r)h^2_{\mathrm{FF}}(x) \approx$$

$$C \underbrace{\operatorname{sinc}^2\left[\frac{2B}{c}r\right]}_{\substack{\text{range sinc with}\\ \text{chirp resolution}}} \underbrace{\operatorname{sinc}^2\left[\frac{2T_b f_c V}{Hc}x\right]}_{\substack{\text{azimuth sinc with}\\ \text{UF-SAR resolution}}}$$

$$\sum_n \underbrace{\operatorname{sinc}^2\left[T\frac{2f_cV}{Hc}\left(x - \overbrace{n\frac{Hc\mathrm{BRF}}{2f_cV}}^{\text{target copy positions}}\right)\right]}_{\substack{\text{repeated azimuth sincs with}\\ \text{FF-SAR resolution}}},$$

$$W_c(r) \approx C \int \mathrm{dz}\; p(z)$$

$$\int \mathrm{dy} \int \mathrm{dx}\; \frac{G^2(x,y)\sigma_0(x,y)}{r^4} h_c^2(r - R(x,y,z), x), \quad (5)$$

$$W^{\mathrm{multi}}_{\mathrm{UF}}(r) = \sum_{t_b} W_{\mathrm{UF}}(r) \approx C \int \mathrm{dz}\; p(z) \int \mathrm{dy}\; G_y^2(y)$$

$$\int \mathrm{dx} \underbrace{\sum_{t_b} G_x^2(x) h^2_{\mathrm{UF}}(r - R(x,y,z), x; x_l = Vt_b)}_{=I_{\mathrm{UF}}(x,y,z)},$$

$$I_{\mathrm{UF}}(x,y,z) \to \operatorname{sinc}^2\left[\frac{x}{L_x}\right] \sum_{t_b} G_x^2(Vt_b + x)$$

$$\operatorname{sinc}^2\left[\frac{2B}{c}\left(r - r_0(y,z) - \left(\frac{xV}{H}t_b + \frac{x^2}{2H} - \frac{xf_cV}{Hs}\right)\right)\right]$$

$$= \mathcal{T}_{\mathrm{UF}}(r - r_0, x),$$

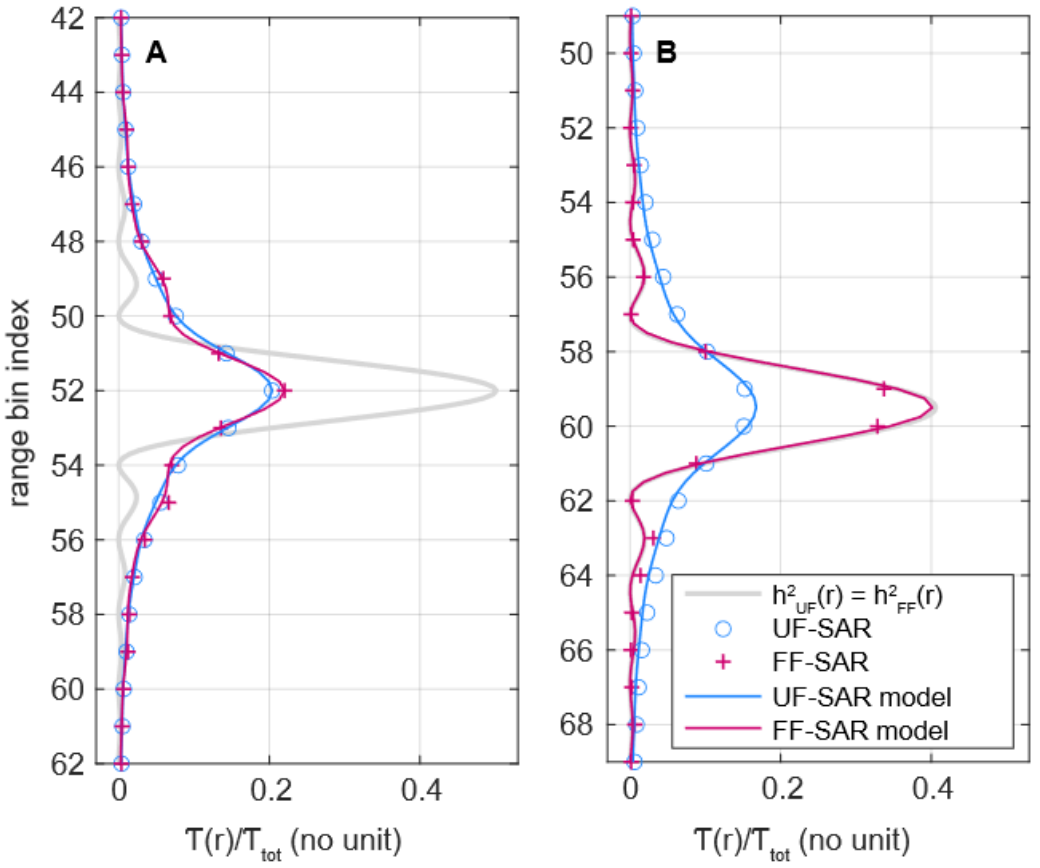

Fig. 10. Comparison of transponder images from Figs. 4 and 6 with IRF models from Eqs. 8 and 13 in terms of the flat line response $\mathcal{T}(r - r_0)$ for Sentinel-3 (panel A) and Sentinel-6 (panel B). The range offset r_0 was manually adjusted to represent the data best. Differences between UF-SAR and FF-SAR ocean waveforms are entirely governed by differences between these functions, when sea surface motion is neglected. The legend regards both panels.

Synthetic aperture and along-track resolution - Theory

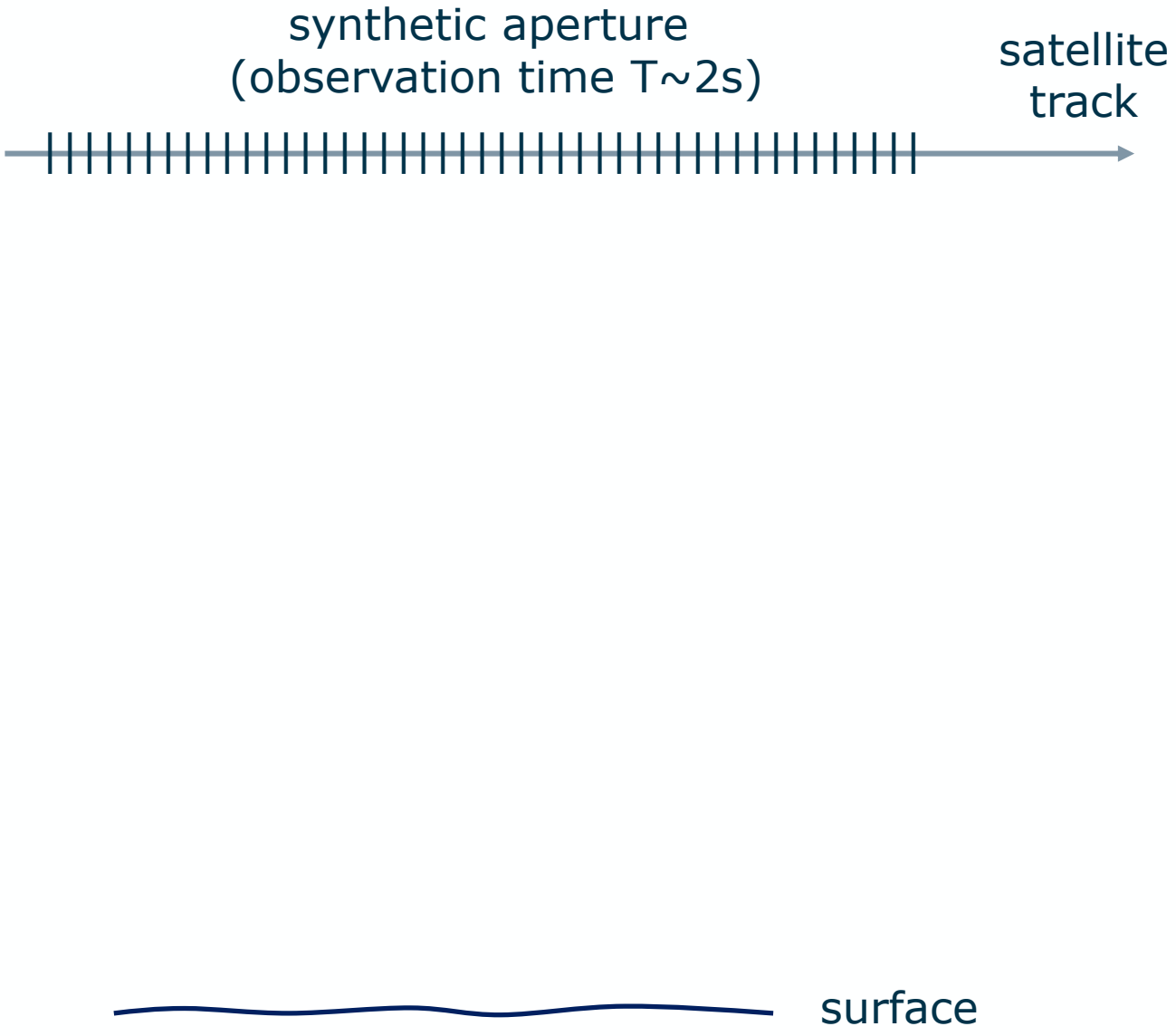

Synthetic aperture and along-track resolution - Theory

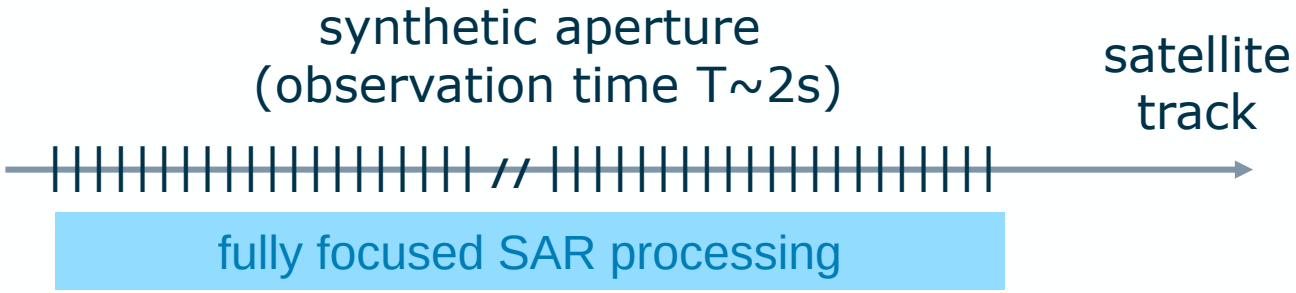

We can do the focusing over the whole aperture T. As in the FFT, the frequency resolution is then proportional to 1/T, about ~0.5 m along track distance for S3.

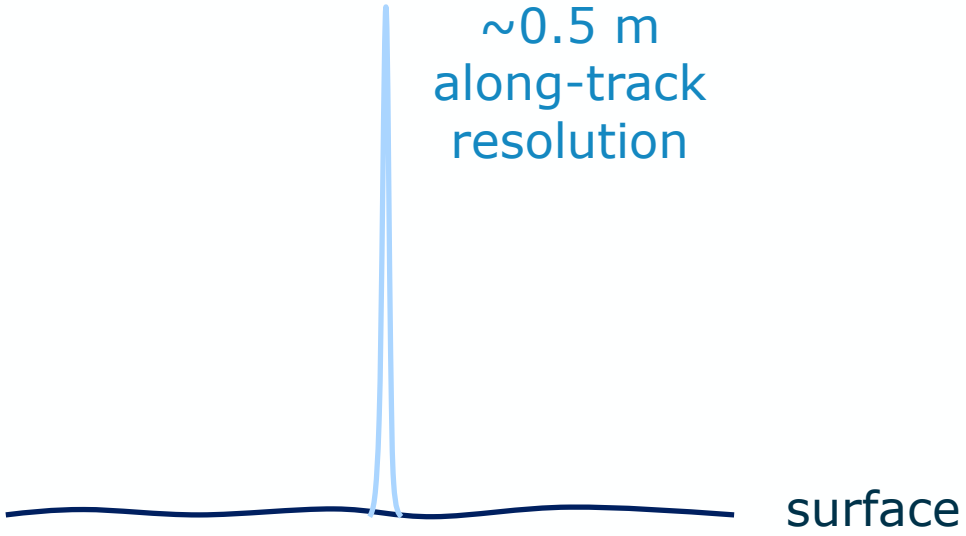

Synthetic aperture and along-track resolution - Theory

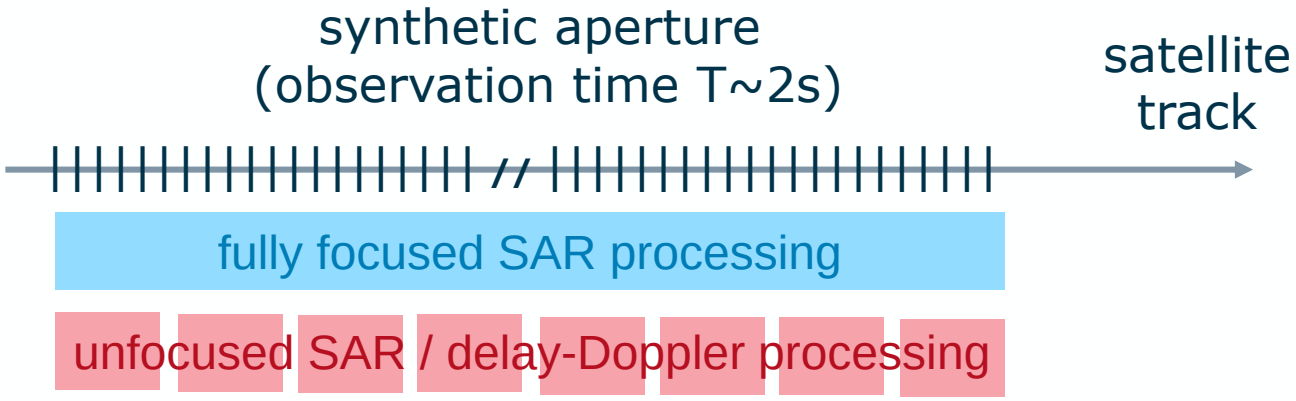

We can do the focusing over the whole aperture T. As in the FFT, the frequency resolution is then proportional to 1/T, about ~0.5 m along track distance for S3.

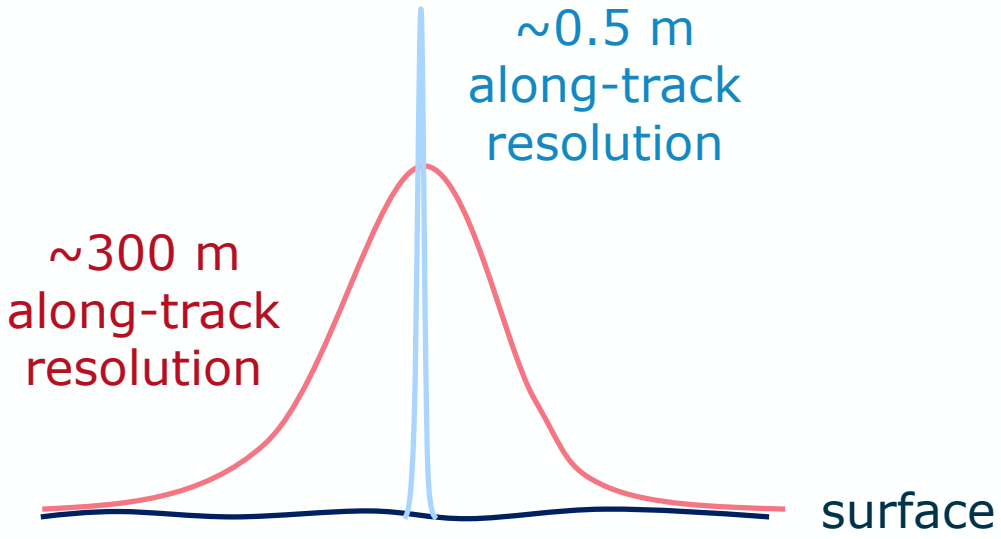

However, we can also subdivide the pulses into N chunks beforehand and on each perform the FFT, which is then averaged. The frequency resolution is then proportional to 1/(NT), about ~300 m along track distance for single S3 bursts with duration ~3.5 ms.

Egido et al. (2017), 10.1109/TGRS.2016.2607122

Synthetic aperture and along-track resolution

Sentinel-6 Michael Freilich

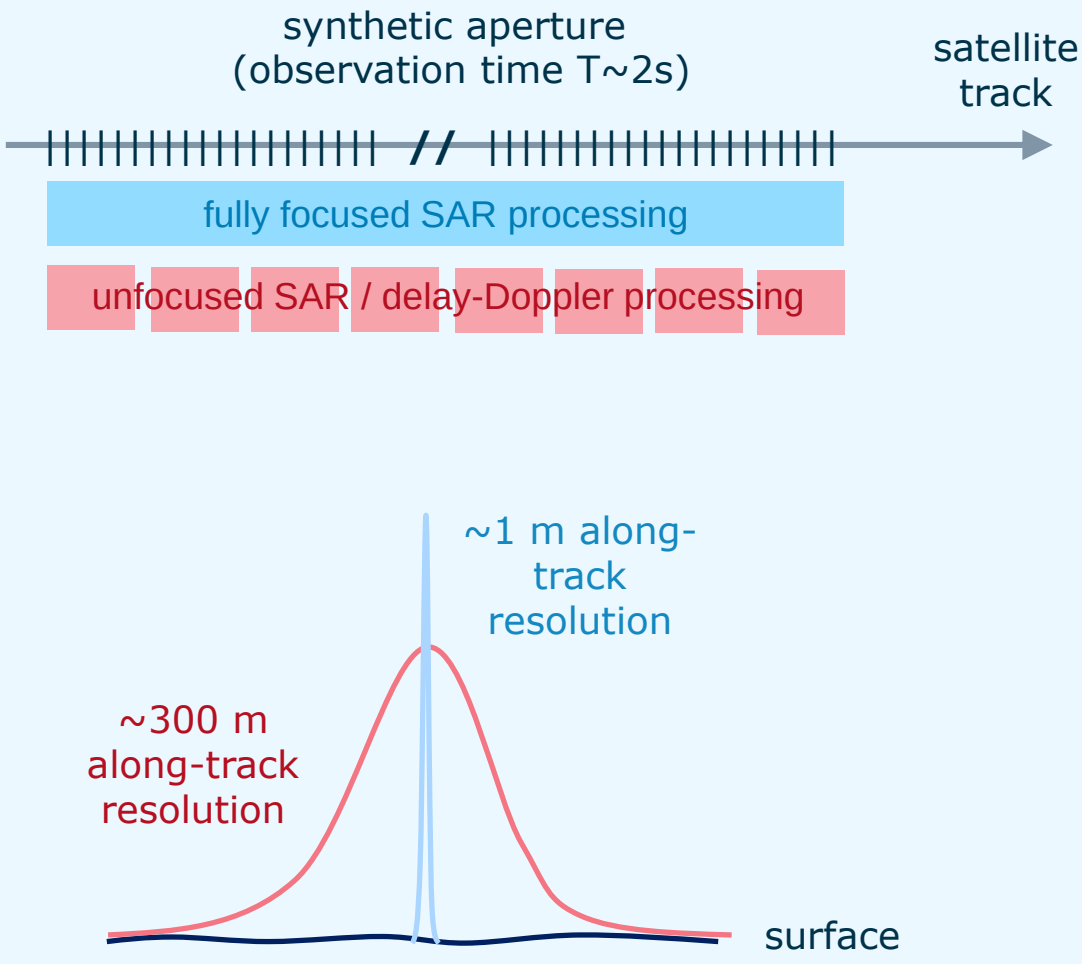

CryoSat-2 & Sentinel-3